TÉCNICO LISBOA

Nonlinear Control of Multi-Quadrotor Flight Formations

Diogo Gomes Farinha dos Santos Ferreira

Thesis to obtain the Master of Science Degree in

Aerospace Engineering

Supervisors: Professor Dr. Afzal Suleman
Professor Dr. Paulo Jorge Coelho Ramalho Oliveira

Examination Committee

Chairperson: Prof. Dr. Filipe Szolnoky Ramos Pinto Cunha
Supervisor: Professor Dr. Paulo Jorge Coelho Ramalho Oliveira
Member of the Committee: Professor Dr. João Manuel Lage de Miranda Lemos

December 2021

In loving memory of my Grandmother.

Acknowledgments

This work would never have been possible without the help of many, to whom I am deeply grateful. A special thank you is due to my supervisors for their guidance and insights. Lastly, to my parents and brother, who have been behind me through thick and thin.

Resumo

O objetivo deste trabalho é desenvolver um sistema de controlo com base em métodos de controlo moderno para controlar grupos de veículos aéreos não tripulados quadrirrotores em voo em formacão. É implementada uma metodologia de seguimento de líder onde um veículo líder possui uma trajetória definida e os veículos seguidores são controlados de modo a seguir o líder mantendo um deslocamento constante.

A solucão para o sistema de controlo, responsável pela formacão de veículos, considera, num primeiro momento, apenas o movimento a altitude constante e, posteriormente, o movimento tridimensional. Em ambos os casos, são derivadas leis de controlo não linear com recurso à teoria de estabilidade de Lyapunov e método de *Backstepping*. As leis de controlo são validadas em simulacão recorrendo a um ambiente e modelos realistas dos veículos.

Palavras-chave: Quadrirrotor, Voo em Formacão, Estabilidade de Lyapunov, Método de Backstepping.

Abstract

The aim of this work is to design a control system based on modern control methods to control flight formations of quadrotor unmanned aerial vehicles. A leader-follower methodology is implemented where the leader vehicle has some predefined trajectory and the follower vehicles are controlled in order to track the leader keeping a constant displacement.

The formation control system, responsible for the vehicle formation, considers, at first, only the motion at constant height, and secondly, the three-dimensional motion. In both cases, the nonlinear control laws are derived based on Lyapunov stability theory and the Backstepping method. The control laws are validated in simulation resorting to a realistic environment and vehicle models.

Keywords: Quadrotor, Formation Flight, Lyapunov Stability, Backstepping Method.

Contents

List of Tables

List of Figures

List of Symbols

Arabic symbols

$\mathbf{0}_{i\times j}$ Null matrix of size $i \times j$.

Greek symbols

Δ Displacement vector.

θ Pitch angle.

λ Vector of Euler angles.

ϕ Roll angle.

ψ Yaw angle.

ω Angular speed.

Ω_i Angular speed of the ith rotor.

Roman symbols

$\{B\}$ Body frame.

c_Q Coefficient of torque.

c_T Coefficient of thrust.

$\mathbf{e}_i$ ith base vector.

$\mathbf{f}$ Total force vector.

g Gravitational acceleration.

$\{I\}$ Inertial frame.

$\mathbf{I}_n$ Identity matrix of size n.

$\mathbf{J}$ Quadrotor inertia tensor.

m Quadrotor mass.

$\mathbf{n}$ Total torque vector.

$\mathbf{p}$	Position vector.
p	Roll speed.
q	Pitch speed.
r	Yaw speed.
$\mathbf{R}$	Rotation matrix form body to inertial frames.
$\mathbf{S}$	Skew-symmetric matrix.
T	Total thrust force.
T_i	Thrust force produced by the ith rotor.
u, v, w	Velocity Cartesian components.
$\mathbf{v}$	Velocity vector.
x, y, z	Position Cartesian components.

Subscripts

ref	Reference value.

Superscripts

$\cdot$	Derivative with respect to time.
B	Expressed in body frame.
I	Expressed in inertial frame.
T	Transpose.

Chapter 1

Introduction

Unmanned Aerial Vehicles (UAVs), also commonly known as drones, were developed through the twentieth century, originally for military purposes. The first applications were during World War II even though those drones were little more than rudimentary remote-controlled airplanes. The Vietnam War, where thousands of American airmen were killed or captured, was a trigger for the rapid development of more sophisticated UAVs for combat missions. In the aftermath of the Six-Day War, Israel developed their first UAVs, which were then successfully deployed in the Operation Peace for Galilee during the 1982 Lebanon War, which resulted in no crewed aircrafts downed. In the twenty-first century, as the technology improved and costs fell, UAVs have been devoted to a myriad of other uses apart from military high-risk missions, ranging from aerial photography, goods delivery, agriculture, mapping and surveillance, pollution monitoring, infrastructure inspections or entertainment.

As of today, if a single UAV can be completely autonomous on a solo mission, a swarm of UAVs can perform much more complex tasks with gains in efficiency and robustness. As an example, [1] describes how it is possible to deploy two UAVs to cooperatively carry heavy loads. [2] presents a strategy for area exploration and mapping carried out by a swarm of autonomous UAVs. For policing and surveillance missions in areas where the communication range is limited, [3] discusses how efficient a network of UAVs can be in covering the area. Also, an algorithm is developed by [4] for swarms of UAVs that maximises the detection of intruders over a certain area. For agriculture applications, [5] delves deeply into the advantages of using multiple UAVs with distributed control for better performance.

1.1 Motivation

Most of the examples shown in § 1 apply different concepts of formation and resort to different techniques of how to control it. The control structure can be either centralised or decentralised. The centralised solutions rely on only one agent performing all computations and assigning the other agents their respective tasks. The centralised algorithms are generally easier to design but

more difficult to implement due to the heavy computational burden. Also, the communication is critical as [6] considers that if the communication link between the central agent and any other agent fails, the entire formation is broken.

The decentralised solutions break down the computational burden into smaller problems to be solved by each of the agents. In this case, the control laws are derived for each agent or subgroup of agents. The decentralised algorithms are expectedly more intricate to design but their implementation is more reliable, efficient and robust.

As far as the formation control problem is concerned there are many different approaches. The most relevant ones are the leader-follower, the virtual leader and the behaviour based. The simplest approach is the leader-follower, which implies the existence of one leader and one or more followers. A formation is achieved when each follower drives into the desired position with respect to the leader, which has some known trajectory. The main disadvantage of this strategy, suggested by [7], is that there is no feedback on the state of the formation as the followers blindly follow the leader.

Another formation control strategy is called the virtual leader approach. In this strategy, the virtual leader describes a reference trajectory and the formation is achieved when all the vehicles in the swarm follow the leader in a rigid structure, maintaining a rigid geometric shape with respect to one another and to a reference frame. The main advantage is that guidance algorithms are simplified because of the fact that the formation can be deemed a rigid body. However, the formation lacks flexibility so complex obstacle avoidance manoeuvres become compromised, as pointed out by [8]. It is of interest especially for guidance and control of spacecraft formations, as done by [9].

The behaviour-based formation control approach defines different control behaviours for different situations of interest such as target tracking or obstacle avoidance. The control action for each vehicle is a weighted average of the control for each behaviour. The work reported in [10] provides further insights into this topic.

In terms of sensing capability and interaction topology of the formation, [11] identifies three distinctions:

- position-based control: each agent has full sensing capability and can drive itself to the desired position with respect to a global reference frame. This approach does not need much interaction among the agents but it might be costly for the advanced sensing technology each agent has to be equipped with, such as GPS receivers.

- displacement-based control: each agent knows the relative position of its neighbours with respect to a global reference frame.

- distance-based control: each agent knows the relative position of its neighbours with respect to its local reference frame. The formation is treated as a rigid body and it is economical on the global information it needs. However, interaction between agents is maximum.

1.2 State of the art

When it comes to developing control solutions for multiple unmanned aerial vehicles flying in formation, one of the problems to be addressed is the consensus problem. According to [12], one of the consensus pioneers, cited by [13], "in networks of agents or dynamic systems, consensus means to reach an agreement regarding a certain quantity of interest that depends on the state of all agents". In other words, this implies that all the vehicles involved agree on some common parameter when they converge to a formation. The consensus problems can be distinguished between unconstrained and constrained. Still according to [13], in unconstrained consensus the state of all agents become equal, whereas in constrained solutions the state of all agents converge to an explicitly defined function. A simple example of an unconstrained consensus is achieved when all vehicles converge to a rigid geometric form. Articles [14] and [15] provide a pedagogical approach and survey of applications of consensus to multi-agent control and article [16], from a recognised authority on the consensus field, analyses three fundamental algorithms with in-depth.

The work in [17] provides a state-of-the-art decentralised cooperative control solution. In this work, the authors coordinate a swarm of vehicles where each has an independent, deterministic and time-dependent path. Also, the vehicles are assumed to arrive at their respective destinations at the same time following a collision-free path. The communication network established between the agents must be bidirectional with no time delay. However, it can be time varying, thereby taking into account temporary breakdowns in the communication links or changing communication topologies along the way. The coordination task is achieved by reaching consensus on a common variable that is the virtual time [18]. The virtual time is a function that maps the universal (clock) time to the mission time of each agent. The control of this variable ensures each agent executes its mission at its own pace and coordinates with its neighbours.

1.3 Objectives

The aim of this work is to design a controller based on modern control methods to control a quadrotor UAV and drive it into a formation. It was chosen a leader-follower approach in which a leader has some predefined trajectory and a follower is controlled in order to track the leader keeping a constant displacement in its reference frame. The formation control solution is done in two steps: firstly, considering only the motion at constant height, secondly, considering the three-dimensional motion. In both cases, the nonlinear control laws are derived based on Lyapunov stability and the backstepping method.

1.4 Thesis Outline

This work is made up of four different chapters.

Chapter 1 is the introduction to the topic of formation control. It begins with a brief history of unmanned aerial vehicles and their usefulness and applications. Section 1.1 highlights different

concepts of formation and control techniques; section 1.2 describes in further detail one state-of-the-art solution; section 1.3 announces the objectives of this work and section 1.4 presents the content of each chapter and section.

Chapter 2 contains the development of the solution. Section 2.1 is for the presentation of the quadrotor kinematics and dynamics; section 2.2 contains the derivations of the control law for the bidirectional motion and the stability of the formation and section 2.3 derives a controller for the three-dimensional motion.

Chapter 3 comprises the simulation results of the algorithms developed. Section 3.1 contains the results for the bidirectional motion and section 3.2 presents the results for the three-dimensional motion.

Chapter 4 draws the main conclusions of the work and section 4.1 presents possible avenues for future developments.

Chapter 2

Formation control

2.1 Quadrotor model

2.1.1 Kinematics

Let $\{I\}$ be an orthonormal reference frame according to the North-East-Down (NED) coordinate system, fixed at some point constant along the time with the orthonormal basis

$$\left\{\mathbf{e}_1 = \begin{pmatrix}1 & 0 & 0\end{pmatrix}^T, \mathbf{e}_2 = \begin{pmatrix}0 & 1 & 0\end{pmatrix}^T, \mathbf{e}_3 = \begin{pmatrix}0 & 0 & 1\end{pmatrix}^T\right\}.$$

Let $\{B\}$ be another orthonormal reference frame centred at point $\mathbf{p} := x\mathbf{e}_1 + y\mathbf{e}_2 + z\mathbf{e}_3$. The orientation of $\{B\}$ with respect to $\{I\}$ is given by the roll, pitch and yaw angles $\lambda := (\phi, \theta, \psi)$ that represent the rotation about their respective axes. The rotation matrix from $\{B\}$ to $\{I\}$ is given by the orthogonal matrix

$$\mathbf{R} := \mathbf{R}(\lambda) \in \mathrm{SO}(3) \triangleq \left\{X \in \mathbb{R}^{3\times 3} : XX^T = X^TX = \mathbf{I}_3, |X| = 1\right\} \tag{2.1}$$

that can be decomposed into three consecutive elementary rotations as

$$\begin{aligned}
\mathbf{R} &= \mathbf{R}_z(\psi)\mathbf{R}_y(\theta)\mathbf{R}_x(\phi) \\
&= \begin{pmatrix}\cos\psi & -\sin\psi & 0\\ \sin\psi & \cos\psi & 0\\ 0 & 0 & 1\end{pmatrix}\begin{pmatrix}\cos\theta & 0 & \sin\theta\\ 0 & 1 & 0\\ -\sin\theta & 0 & \cos\theta\end{pmatrix}\begin{pmatrix}1 & 0 & 0\\ 0 & \cos\phi & -\sin\phi\\ 0 & \sin\phi & \cos\phi\end{pmatrix} \\
&= \begin{pmatrix}\cos\theta\cos\psi & \sin\phi\sin\theta\cos\psi - \cos\phi\sin\psi & \cos\phi\sin\theta\cos\psi + \sin\phi\sin\psi\\ \cos\theta\sin\psi & \sin\phi\sin\theta\sin\psi + \cos\phi\cos\psi & \cos\phi\sin\theta\sin\psi - \sin\phi\cos\psi\\ -\sin\theta & \sin\phi\cos\theta & \cos\phi\cos\theta\end{pmatrix}.
\end{aligned} \tag{2.2}$$

From the definition in (2.1) we can write

$$\begin{aligned} &\mathbf{R}\mathbf{R}^T = \mathbf{I}_3 \\ \Leftrightarrow &\dot{\mathbf{R}}\mathbf{R}^T + \mathbf{R}\dot{\mathbf{R}}^T = 0 \\ \Leftrightarrow &\dot{\mathbf{R}}\mathbf{R}^T = -(\dot{\mathbf{R}}\mathbf{R}^T)^T. \end{aligned} \tag{2.3}$$

Thus, $\dot{\mathbf{R}}\mathbf{R}^T$ is skew-symmetric. Defining the skew-symmetric matrix $\mathbf{S}({}^I\omega) = \dot{\mathbf{R}}\mathbf{R}^T$ the derivative $\dot{\mathbf{R}}$ can be computed as

$$\dot{\mathbf{R}} = \mathbf{S}({}^I\omega)\mathbf{R}, \tag{2.4}$$

where ${}^I\omega \in \mathbb{R}^3$ is the angular velocity of $\{B\}$ expressed in $\{I\}$. Taking into account the property of skew-symmetric matrices that states $\mathbf{R}\mathbf{S}(x) = \mathbf{S}(\mathbf{R}x)\mathbf{R}$ for any $x \in \mathbb{R}^3$, we can write $\dot{\mathbf{R}}$ with the angular velocity ω expressed in $\{B\}$ as

$$\dot{\mathbf{R}} = \mathbf{R}\mathbf{S}(\omega). \tag{2.5}$$

To compute ω we derive $\dot{\mathbf{R}}$ following the elementary rotations:

$$\begin{aligned} \dot{\mathbf{R}} &= \dot{\mathbf{R}}_z\mathbf{R}_y\mathbf{R}_x + \mathbf{R}_z\dot{\mathbf{R}}_y\mathbf{R}_x + \mathbf{R}_z\mathbf{R}_y\dot{\mathbf{R}}_x \\ &= \mathbf{R}_z\mathbf{S}(\dot{\psi}\mathbf{e}_3)\mathbf{R}_y\mathbf{R}_x + \mathbf{R}_z\mathbf{R}_y\mathbf{S}(\dot{\theta}\mathbf{e}_2)\mathbf{R}_x + \mathbf{R}_z\mathbf{R}_y\mathbf{R}_x\mathbf{S}(\dot{\phi}\mathbf{e}_1) \\ &= \mathbf{R}_z\mathbf{R}_y\mathbf{R}_x\mathbf{S}(\mathbf{R}_x^T\mathbf{R}_y^T\dot{\psi}\mathbf{e}_3) + \mathbf{R}_z\mathbf{R}_y\mathbf{R}_x\mathbf{S}(\mathbf{R}_x^T\dot{\theta}\mathbf{e}_2) + \mathbf{R}_z\mathbf{R}_y\mathbf{R}_x\mathbf{S}(\dot{\phi}\mathbf{e}_1) \\ &= \mathbf{R}\mathbf{S}(\underbrace{\dot{\phi}\mathbf{e}_1 + \mathbf{R}_x^T\dot{\theta}\mathbf{e}_2 + \mathbf{R}_x^T\mathbf{R}_y^T\dot{\psi}\mathbf{e}_3}_{\omega}). \end{aligned} \tag{2.6}$$

So the angular velocity is given by

$$\omega = \mathbf{Q}(\lambda)^{-1}\dot{\lambda} = \begin{pmatrix} 1 & 0 & -\sin\theta \\ 0 & \cos\phi & \sin\phi\cos\theta \\ 0 & -\sin\phi & \cos\phi\cos\theta \end{pmatrix} \begin{pmatrix} \dot{\phi} \\ \dot{\theta} \\ \dot{\psi} \end{pmatrix}. \tag{2.7}$$

Let $\mathbf{p}$ be the quadrotor's position and $\mathbf{v} := u\mathbf{e}_1 + v\mathbf{e}_2 + w\mathbf{e}_3$ its velocity in $\{I\}$. The kinematics of the rigid body, for any $\theta \neq (2k+1)\frac{\pi}{2}$, $\forall\, k \in \mathbb{Z}$, can be written as

$$\begin{cases} \dot{\mathbf{p}} = \mathbf{v} \\ \dot{\lambda} = \mathbf{Q}(\lambda)\omega \end{cases} \tag{2.8}$$

with

$$\mathbf{Q}(\lambda) = \begin{pmatrix} 1 & \sin\phi\tan\theta & \cos\phi\tan\theta \\ 0 & \cos\phi & -\sin\phi \\ 0 & \frac{\sin\phi}{\cos\theta} & \frac{\cos\phi}{\cos\theta} \end{pmatrix}. \tag{2.9}$$

2.1.2 Dynamics

Let m be the mass of the quadrotor and $\mathbf{J} \in \mathbb{R}^{3\times3}$ its inertia tensor. Newton's second law states the conservation of linear and angular momentum in inertial frames. For the translation motion, the sum of all external forces is

$$^{I}\mathbf{f} = \frac{\mathrm{d}}{\mathrm{d}t}(m\mathbf{v}) = m\dot{\mathbf{v}}. \tag{2.10}$$

For the angular motion, the sum of all external moments is

$$^{I}\tau = \frac{\mathrm{d}}{\mathrm{d}t}(\mathbf{R}\mathbf{J}\omega) = \mathbf{R}\mathbf{J}\dot{\omega} + \mathbf{R}\mathbf{S}(\omega)\mathbf{J}\omega. \tag{2.11}$$

If $\mathbf{n} = \mathbf{R}^{T}\,{}^{I}\tau \in \mathbb{R}^3$ is the sum of all external moments expressed in $\{B\}$, the rotational dynamics is

$$\mathbf{n} = \mathbf{J}\dot{\omega} + \mathbf{S}(\omega)\mathbf{J}\omega. \tag{2.12}$$

The complete dynamics of the rigid body in $\{I\}$ is given by

$$\begin{cases} m\dot{\mathbf{v}} = \mathbf{f} \\ \mathbf{J}\dot{\omega} = -\mathbf{S}(\omega)\mathbf{J}\omega + \mathbf{n} \end{cases}. \tag{2.13}$$

A quadrotor is made of two pairs of counter-rotating rotors, assumed equal and equally spaced, as represented in figure 2.1. The forces applied on the quadrotor include its weight, aligned with the inertial frame z axis pointing downwards, and the total thrust force $T = \sum_{i=1}^{4} T_i$, along the body z axis, pointing upwards. Relative to $\{I\}$, it is given by

$$\mathbf{f} = mg\mathbf{e}_3 - T\mathbf{R}\mathbf{e}_3. \tag{2.14}$$

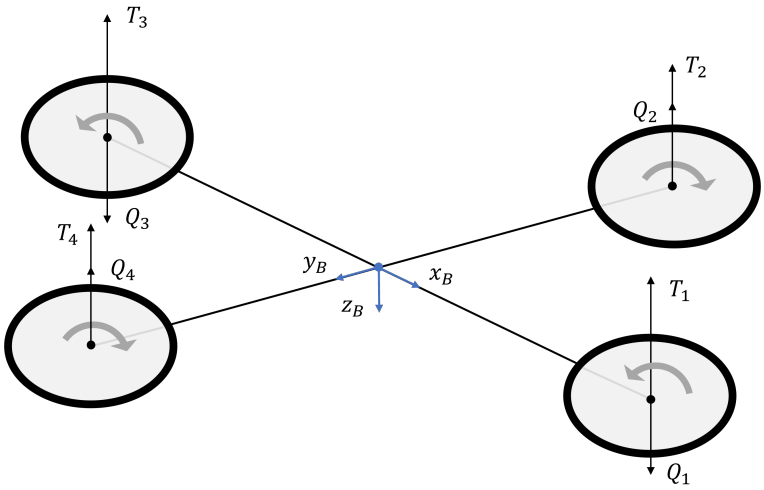

Figure 2.1: Simplified representation of a quadrotor with forces and moments on each rotor

The moments applied on the quadrotor are originated from the different thrust forces produced

by each rotor and the reaction torque generated by the rotors rotating. If l is the quadrotor radius, i.e. the distance between the centre of mass and the centre of each rotor, the moments about x and y can be written as

$$n_x = l(T_2 - T_4); \quad n_y = l(T_1 - T_3). \tag{2.15}$$

For the purpose of this work, which by no means intends to be a fastidious description of the quadrotor dynamics, the thrust force and reaction torque of each rotor are assumed proportional to its angular speed squared, such that

$$T_i = c_T \Omega_i^2; \quad Q_i = (-1)^{i+1} c_Q \Omega_i^2. \tag{2.16}$$

The sum of all external moments relative to $\{B\}$ is

$$\mathbf{n} = \begin{pmatrix} 0 & l & 0 & -l \\ l & 0 & -l & 0 \\ c_Q/c_T & -c_Q/c_T & c_Q/c_T & -c_Q/c_T \end{pmatrix} \begin{pmatrix} T_1 \\ T_2 \\ T_3 \\ T_4 \end{pmatrix}. \tag{2.17}$$

2.2 2D motion

As a first attempt towards our objective of controlling a formation, we first restrict the problem to the two-dimensional motion of the quadrotor in the xOy plane, which is equivalent to considering the motion at constant height. In what follows, a controller will be designed to drive a simplified quadrotor model to its desired position and a formation system consisting of one leader and one follower will be studied.

2.2.1 Simplified quadrotor model

Let $\mathbf{p} := x\mathbf{e}_1 + y\mathbf{e}_2$ be the quadrotor's position, $\mathbf{v} := u\mathbf{e}_1 + v\mathbf{e}_2$ its velocity expressed in $\{B\}$ and r its angular velocity expressed in $\{B\}$. We can simplify equation (2.8) to obtain the horizontal kinematics as

$$\begin{cases} \dot{x} = u\cos\psi - v\sin\psi \\ \dot{y} = u\sin\psi + v\cos\psi \\ \dot{\psi} = r \end{cases}, \tag{2.18}$$

with only two independent equations. Given that we ultimately wish to control the force (proportional to the linear acceleration) and the torque (proportional to the angular acceleration), it is wise to select the control vector $(\dot{u}, \dot{r})^T$ (or alternatively $(\dot{v}, \dot{r})^T$). So the kinematics can also be written as

$$\begin{cases} \dot{\mathbf{p}} = \mathbf{R}\mathbf{v} \\ \dot{\psi} = r \end{cases}, \tag{2.19}$$

where $\mathbf{v} := v\mathbf{e}_1$ is the horizontal velocity and $\mathbf{R}$ is the rotation matrix from the body-fixed reference frame to the inertial reference frame, given by

$$\mathbf{R} \triangleq \mathbf{R}(\psi) = \begin{pmatrix} \cos\psi & -\sin\psi \\ \sin\psi & \cos\psi \end{pmatrix}. \tag{2.20}$$

2.2.2 Trajectory tracking controller

We want the follower to track the leader keeping a constant offset in the follower's reference frame. If $\mathbf{p} \in \mathbb{R}^2$ is the follower's position and $\mathbf{c} \in \mathbb{R}^2$ the leader's position, $\mathbf{c}-\mathbf{p}$ is the leader's position in the follower's reference frame, written in the inertial reference frame. If $\Delta := \begin{pmatrix} \Delta_x & \Delta_y \end{pmatrix}^T$ is the desired displacement, we can write the position error $\mathbf{z}_1 \in \mathbb{R}^2$ expressed in the follower's reference frame as

$$\mathbf{z}_1 = \mathbf{R}^T(\mathbf{c}-\mathbf{p}) - \Delta. \tag{2.21}$$

The error dynamics can be computed as

$$\begin{aligned} \dot{\mathbf{z}}_1 &= \mathbf{R}^T(\dot{\mathbf{c}}-\dot{\mathbf{p}}) + \dot{\mathbf{R}}^T(\mathbf{c}-\mathbf{p}) \\ &= \mathbf{R}^T\dot{\mathbf{c}} - \mathbf{v} - \mathbf{S}(r)\mathbf{R}^T(\mathbf{c}-\mathbf{p}) \\ &= \mathbf{R}^T\dot{\mathbf{c}} - \mathbf{v} - \mathbf{S}(r)(\mathbf{z}_1+\Delta). \end{aligned} \tag{2.22}$$

An equilibrium point $\mathbf{z}_e \in \mathbb{R}^2$ for the error system above makes $\dot{\mathbf{z}}_1 = 0$ and is given by

$$\mathbf{z}_e = \mathbf{S}(r)^{-1}\left[\mathbf{R}^T\dot{\mathbf{c}} - \mathbf{v}\right] - \Delta. \tag{2.23}$$

By making the appropriate change of coordinates one can obtain the error system with an equilibrium point at the origin. We now want to derive a control law to stabilise the system around this equilibrium point.

Let $V_1 : \mathbb{R}^2 \to \mathbb{R}$ be a continuously differentiable Lyapunov function such that $V_1(0) = 0$, $V_1(\mathbf{z}_1) > 0$, $\forall \mathbf{z}_1 \neq 0$ and $\|\mathbf{z}_1\| \to \infty \Rightarrow V_1(\mathbf{z}_1) \to \infty$ given by

$$V_1(\mathbf{z}_1) = \frac{1}{2}\|\mathbf{z}_1\|^2, \tag{2.24}$$

with its derivative computed as

$$\begin{aligned} \dot{V}_1(\mathbf{z}_1) &= \mathbf{z}_1^T\dot{\mathbf{z}}_1 \\ &= \mathbf{z}_1^T\left(\mathbf{R}^T\dot{\mathbf{c}} - \mathbf{v} - \mathbf{S}(r)(\mathbf{z}_1+\Delta)\right) \\ &= \mathbf{z}_1^T\left(\mathbf{R}^T\dot{\mathbf{c}} - \mathbf{v} - \mathbf{S}(r)\Delta\right). \end{aligned} \tag{2.25}$$

The control variables are not visible yet so we should continue with the backstepping method. This method can be used to stabilise systems written in strict-feedback form, according to [19]. If we

now add and subtract a term $k_1\|\mathbf{z}_1\|^2$, we get

$$\begin{aligned}\dot{V}_1(\mathbf{z}_1) &= -k_1\|\mathbf{z}_1\|^2 + \mathbf{z}_1^T \underbrace{\left[k_1\mathbf{z}_1 + \mathbf{R}^T\dot{\mathbf{c}} - \mathbf{v} - \mathbf{S}(r)\Delta\right]}_{\mathbf{z}_2} \\ &= -k_1\|\mathbf{z}_1\|^2 + \mathbf{z}_1^T\mathbf{z}_2,\end{aligned} \tag{2.26}$$

where another error $\mathbf{z}_2 \in \mathbb{R}^2$ was introduced. To apply backstepping with one step we define the continuously differentiable augmented Lyapunov function $V_2 : \mathbb{R}^4 \to \mathbb{R}$ such that $V_2(0) = 0$, $V_2(\mathbf{z}_1, \mathbf{z}_2) > 0$, $\forall(\mathbf{z}_1, \mathbf{z}_2) \neq 0$ and $\|(\mathbf{z}_1, \mathbf{z}_2)\| \to \infty \Rightarrow V_2(\mathbf{z}_1, \mathbf{z}_2) \to \infty$ given by

$$V_2(\mathbf{z}_1, \mathbf{z}_2) = V_1(\mathbf{z}_1) + \frac{1}{2}\|\mathbf{z}_2\|^2, \tag{2.27}$$

and its derivative computed as

$$\begin{aligned}\dot{V}_2(\mathbf{z}_1, \mathbf{z}_2) &= \dot{V}_1 + \mathbf{z}_2^T\dot{\mathbf{z}}_2 \\ &= \dot{V}_1 + \mathbf{z}_2^T\left[k_1\dot{\mathbf{z}}_1 + \mathbf{R}^T\ddot{\mathbf{c}} - \mathbf{S}(r)\mathbf{R}^T\dot{\mathbf{c}} - \dot{\mathbf{v}} - \mathbf{S}(\dot{r})\Delta\right] \\ &= \dot{V}_1 + \mathbf{z}_2^T\left[k_1\dot{\mathbf{z}}_1 + \mathbf{R}^T\ddot{\mathbf{c}} - \mathbf{S}(r)\mathbf{R}^T\dot{\mathbf{c}} - \begin{pmatrix}\dot{v}\\0\end{pmatrix} - \begin{pmatrix}0 & -\dot{r}\\ \dot{r} & 0\end{pmatrix}\begin{pmatrix}\Delta_x\\\Delta_y\end{pmatrix}\right] \\ &= \dot{V}_1 + \mathbf{z}_2^T\left[k_1\dot{\mathbf{z}}_1 + \mathbf{R}^T\ddot{\mathbf{c}} - \mathbf{S}(r)\mathbf{R}^T\dot{\mathbf{c}} - \begin{pmatrix}1 & -\Delta_y\\ 0 & \Delta_x\end{pmatrix}\begin{pmatrix}\dot{v}\\\dot{r}\end{pmatrix}\right].\end{aligned} \tag{2.28}$$

From equation (2.28) we could isolate the linear acceleration $\dot{v}$ and angular acceleration $\dot{r}$. We can now derive a control law for $\begin{pmatrix}\dot{v} & \dot{r}\end{pmatrix}^T$, considered as inputs, such that the derivative of the augmented Lyapunov function (2.28) is negative definite. That control law should be

$$\begin{pmatrix}\dot{v}\\\dot{r}\end{pmatrix} = \begin{pmatrix}1 & -\Delta_y\\ 0 & \Delta_x\end{pmatrix}^{-1}\left[k_1\dot{\mathbf{z}}_1 + \mathbf{R}^T\ddot{\mathbf{c}} - \mathbf{S}(r)\mathbf{R}^T\dot{\mathbf{c}} + \mathbf{z}_1 + k_2\mathbf{z}_2\right] \qquad \forall\Delta_x \neq 0. \tag{2.29}$$

Applying the control law from equation (2.29), the error system can be written in strict-feedback form as

$$\begin{cases}\dot{\mathbf{z}}_1 = -\left(\mathbf{S}(r) + k_1\mathbf{I}_2\right)\mathbf{z}_1 + \mathbf{z}_2\\ \dot{\mathbf{z}}_2 = -\mathbf{z}_1 - k_2\mathbf{z}_2\end{cases}, \tag{2.30}$$

where $\mathbf{I}_2$ is the identity matrix of size 2. The derivative of V_2 becomes

$$\dot{V}_2(\mathbf{z}_1, \mathbf{z}_2) = -k_1\|\mathbf{z}_1\|^2 - k_2\|\mathbf{z}_2\|^2. \tag{2.31}$$

It is clear that $\dot{V}_2(\mathbf{z}_1, \mathbf{z}_2) < 0$, $\forall(\mathbf{z}_1, \mathbf{z}_2) \neq 0$ if $k_1 > 0$ and $k_2 > 0$. Thus, according to the Barbashin-Krasovskii theorem [19, theorem 4.2], the error system is globally asymptotically stable around its equilibrium point $(\mathbf{z}_1, \mathbf{z}_2) = 0$.

2.2.3 Perturbed system

In the real world there is no such thing as a physical system unaffected by disturbances. As a result, one should always account for external disturbances and include them in the dynamics. In the present case, we assume the existence of an unknown external disturbance $\mathbf{d} \in \mathbb{R}^2$ expressed in $\{B\}$, such that the dynamics of the error $\mathbf{z}_2$ is

$$\dot{\mathbf{z}}_2 = k_1\dot{\mathbf{z}}_1 + \mathbf{R}^T\ddot{\mathbf{c}} - \mathbf{S}(r)\mathbf{R}^T\dot{\mathbf{c}} - \dot{\mathbf{v}} - \mathbf{S}(\dot{r})\Delta + \mathbf{R}\mathbf{d}. \tag{2.32}$$

Additionally, we assume the controller has an estimator $\hat{\mathbf{d}} \in \mathbb{R}^2$ to estimate $\mathbf{d}$ such that the control law is

$$\begin{pmatrix} \dot{v} \\ \dot{r} \end{pmatrix} = \begin{pmatrix} 1 & -\Delta_y \\ 0 & \Delta_x \end{pmatrix}^{-1} \left[k_1\dot{\mathbf{z}}_1 + \mathbf{R}^T\ddot{\mathbf{c}} - \mathbf{S}(r)\mathbf{R}^T\dot{\mathbf{c}} + \mathbf{z}_1 + k_2\mathbf{z}_2 + \mathbf{R}\hat{\mathbf{d}}\right] \qquad \forall\Delta_x \neq 0. \tag{2.33}$$

With this formulation, the error system is now

$$\begin{cases} \dot{\mathbf{z}}_1 = -\left(\mathbf{S}(r) + k_1\mathbf{I}_2\right)\mathbf{z}_1 + \mathbf{z}_2 \\ \dot{\mathbf{z}}_2 = -\mathbf{z}_1 - k_2\mathbf{z}_2 + \mathbf{R}(\mathbf{d} - \hat{\mathbf{d}}) \end{cases}. \tag{2.34}$$

Expressing the estimation error by $\tilde{\mathbf{d}} = \mathbf{d} - \hat{\mathbf{d}}$ and the error state by $\mathbf{z} = \begin{pmatrix} \mathbf{z}_1 & \mathbf{z}_2 \end{pmatrix}^T$, the error dynamics can be written in state space as

$$\dot{\mathbf{z}} = \underbrace{\begin{pmatrix} -(\mathbf{S}(r) + k_1\mathbf{I}_2) & \mathbf{I}_2 \\ -\mathbf{I}_2 & -k_2\mathbf{I}_2 \end{pmatrix}}_{\mathbf{A}}\mathbf{z} + \underbrace{\begin{pmatrix} \mathbf{0}_{2\times 2} \\ \mathbf{R} \end{pmatrix}}_{\mathbf{B}}\tilde{\mathbf{d}}, \tag{2.35}$$

where matrices $\mathbf{A}$ and $\mathbf{B}$ have been defined.

Now, we wish to design an adaptive controller for the estimator $\hat{\mathbf{d}}$. Let $V_3 : \mathbb{R}^6 \to \mathbb{R}$ be a continuously differentiable Lyapunov function such that $V_3(0) = 0$, $V_3(\mathbf{z}, \tilde{\mathbf{d}}) > 0$, $\forall(\mathbf{z}, \tilde{\mathbf{d}}) \neq 0$ and $\|(\mathbf{z}, \tilde{\mathbf{d}})\| \to \infty \Rightarrow V_3(\mathbf{z}, \tilde{\mathbf{d}}) \to \infty$ given by

$$V_3(\mathbf{z}, \tilde{\mathbf{d}}) = V_2(\mathbf{z}) + \frac{1}{2k_d}\|\tilde{\mathbf{d}}\|^2, \tag{2.36}$$

where $k_d > 0$ is an estimator gain. Its derivative is computed as

$$\begin{aligned} \dot{V}_3(\mathbf{z}, \tilde{\mathbf{d}}) &= \mathbf{z}^T\dot{\mathbf{z}} + \frac{1}{k_d}\tilde{\mathbf{d}}^T\dot{\tilde{\mathbf{d}}} \\ &= \mathbf{z}^T(\mathbf{A}\mathbf{z} + \mathbf{B}\tilde{\mathbf{d}}) + \frac{1}{k_d}\tilde{\mathbf{d}}^T\dot{\tilde{\mathbf{d}}} \\ &= \mathbf{z}^T\mathbf{A}\mathbf{z} + \mathbf{z}^T\mathbf{B}\tilde{\mathbf{d}} + \frac{1}{k_d}\tilde{\mathbf{d}}^T\dot{\tilde{\mathbf{d}}}. \end{aligned} \tag{2.37}$$

The first term of $\dot{V}_3$ is negative for all $\mathbf{z} \neq 0$ as it has already been proved the error system converges

under the control law from equation (2.29). As of the remaining two terms, $\dot{V}_3$ gets negative for all $(\mathbf{z}, \tilde{\mathbf{d}}) \neq 0$ if they sum to zero. So,

$$\begin{aligned} &\mathbf{z}^T\mathbf{B}\tilde{\mathbf{d}} + \frac{1}{k_d}\tilde{\mathbf{d}}^T\dot{\tilde{\mathbf{d}}} = 0 \\ \Leftrightarrow &\dot{\tilde{\mathbf{d}}}^T = -k_d\mathbf{z}^T\mathbf{B}. \end{aligned} \tag{2.38}$$

If the disturbance is assumed constant, then $\dot{\tilde{\mathbf{d}}} = -\dot{\hat{\mathbf{d}}}$, so the adaptation law for the estimator is

$$\dot{\hat{\mathbf{d}}} = k_d\mathbf{B}^T\mathbf{z}. \tag{2.39}$$

Now that we have the tracking control and the disturbance estimation, we must study the stability of the system comprised of both the position error and the disturbance estimation error simultaneously. This system is given by

$$\begin{pmatrix} \dot{\mathbf{z}} \\ \dot{\tilde{\mathbf{d}}} \end{pmatrix} = \begin{pmatrix} \mathbf{A} & \mathbf{B} \\ -k_d\mathbf{B}^T & \mathbf{0}_{2\times 2} \end{pmatrix} \begin{pmatrix} \mathbf{z} \\ \tilde{\mathbf{d}} \end{pmatrix}. \tag{2.40}$$

Let $\Omega = \{(\mathbf{z}, \tilde{\mathbf{d}}) \in \mathbb{R}^6 : V_3(\mathbf{z}, \tilde{\mathbf{d}}) \leq c\}$ for any $c \in \mathbb{R}^+$. The set Ω is compact since V_3 is radially unbounded and, from Lyapunov's direct method [19, theorem 4.1], it is positively invariant with respect to the dynamics (2.40). Let E be the set of all points in Ω where $\dot{V}_3(\mathbf{z}, \tilde{\mathbf{d}}) = 0$. This set is given by

$$E = \{(\mathbf{z}, \tilde{\mathbf{d}}) \in \mathbb{R}^6 : \mathbf{z} = 0\}. \tag{2.41}$$

Let M be the largest invariant set contained in E. By LaSalle's theorem [19, theorem 4.4], every solution with initial condition in Ω approaches M as $t \to \infty$. Since for any $(\mathbf{z}, \tilde{\mathbf{d}}) \in \mathbb{R}^6$ there exists a $c > 0$ such that $(\mathbf{z}, \tilde{\mathbf{d}}) \in \Omega$, we have that any solution converges to M. From its invariance and recalling system (2.35), we have that, for all $(\mathbf{z}, \tilde{\mathbf{d}}) \in M$,

$$\begin{aligned} \dot{\mathbf{z}} = 0 &\Leftrightarrow \mathbf{B}\tilde{\mathbf{d}} = \mathbf{0}_{4\times 1} \\ &\Leftrightarrow \tilde{\mathbf{d}} = \mathbf{0}_{2\times 1}. \end{aligned} \tag{2.42}$$

Therefore, $(\mathbf{z}, \tilde{\mathbf{d}}) = 0$ is the only element in M and the system is globally asymptotically stable around the origin.

2.2.4 Frequency response

We now want to study the frequency response of the system in order to tune the gains k_1, k_2 and k_d. Recalling the dynamics (2.40) we can write

$$\begin{aligned}\dot{\mathbf{z}} &= \mathbf{A}\mathbf{z} + \mathbf{B}\tilde{\mathbf{d}} \\ &= \mathbf{A}\mathbf{z} + \mathbf{B}\mathbf{d} - \mathbf{B}\int \dot{\hat{\mathbf{d}}} \\ &= \mathbf{A}\mathbf{z} + \mathbf{B}\mathbf{d} - k_d\mathbf{B}\int \mathbf{B}^T\mathbf{z}.\end{aligned} \tag{2.43}$$

Under some simplifying conditions, that will be made clear from the context, by taking the Laplace transform on both sides, one can represent the system in the frequency domain as

$$\begin{aligned}s\mathbf{Z}(s) &= \mathbf{A}\mathbf{Z}(s) + \mathbf{B}\mathbf{D}(s) - \frac{k_d}{s}\mathbf{B}\mathbf{B}^T\mathbf{Z}(s) \\ \Leftrightarrow \left(s\mathbf{I}_4 - \mathbf{A} + \frac{k_d}{s}\mathbf{B}\mathbf{B}^T\right)&\mathbf{Z}(s) = \mathbf{B}\mathbf{D}(s).\end{aligned} \tag{2.44}$$

The transfer function from $\mathbf{B}\mathbf{D}(s)$ to $\mathbf{Z}(s)$ is the inverse of the matrix that multiplies $\mathbf{Z}(s)$, when it exists, given by

$$\begin{pmatrix}(s+k_1)\mathbf{I}_2 + \mathbf{S}(r) & -\mathbf{I}_2 \\ \mathbf{I}_2 & (s+k_2)\mathbf{I}_2 + \frac{k_d}{s}\mathbf{R}^2\end{pmatrix}^{-1}. \tag{2.45}$$

This transfer function, as it is defined, depends on the yaw rate r and the yaw angle ψ, which are inputs of the system. If we consider the vehicle describing a linear path heading north, we can set $r = 0 \Rightarrow \mathbf{S}(r) = 0$ and $\psi = 0 \Rightarrow \mathbf{R} = \mathbf{I}_2$. As a result, the transfer function under this assumption is given by

$$\mathbf{H}(s) = \frac{1}{p(s)}\begin{pmatrix}s^2 + k_2 s + k_d & 0 & s & 0 \\ 0 & s^2 + k_2 s + k_d & 0 & s \\ -s & 0 & s(s+k_1) & 0 \\ 0 & -s & 0 & s(s+k_1)\end{pmatrix} \tag{2.46}$$

with

$$p(s) = s^3 + (k_1 + k_2)s^2 + (k_1k_2 + k_d + 1)s + k_1k_d.$$

The transfer function from $\mathbf{D}(s)$ to $\mathbf{Z}(s)$ is given by $\mathbf{H}(s)\mathbf{B}$, taking the form

$$\begin{pmatrix}\mathbf{z}_1 \\ \mathbf{z}_2\end{pmatrix} = \frac{1}{p(s)}\begin{pmatrix}s & 0 \\ 0 & s \\ s(s+k_1) & 0 \\ 0 & s(s+k_1)\end{pmatrix}\begin{pmatrix}d_1 \\ d_2\end{pmatrix}. \tag{2.47}$$

This transfer function is a third-order system that shows the form of a band-pass filter, which means both constant and high-frequency disturbances are attenuated. By tuning the gains we can

narrow the frequency range of allowed disturbances and adjust the filter gain.

Under similar simplifying conditions as before, the transfer function from $\mathbf{d}$ to the position error $\mathbf{z}_1$ is

$$h(s) = \frac{s}{s^3 + (k_1 + k_2)s^2 + (k_1k_2 + k_d + 1)s + k_1k_d}. \tag{2.48}$$

We can first tune the gains k_1 and k_2 by considering the second-order low-pass filter that results from neglecting the disturbance estimation term. In that case, we have

$$h_2(s) = \frac{1}{s^2 + (k_1 + k_2)s + k_1k_2 + 1} = \frac{1}{s^2 + 2\xi\omega_n s + \omega_n^2}. \tag{2.49}$$

The poles can be placed to ensure the desired dynamic behaviour. By defining a damping factor ξ and a natural frequency ω_n, the gains $k_1 > 0$ and $k_2 > 0$ can be computed by comparing with the general second-order system. Afterwards, the gain $k_d > 0$ can be adjusted by analysing a root locus of system (2.48).

2.2.5 Closed-loop system

In the previous sections we have used Lyapunov stability theory to prove global asymptotic stability of the error system. However, validation of the control law has yet to be done to prove stability of the closed-loop system when the errors have converged to zero. From the definition of the error dynamics in equation (2.22), we have, in steady state,

$$\begin{cases} \mathbf{z}_1 = 0 \\ \dot{\mathbf{z}}_1 = 0 \end{cases} \Rightarrow \mathbf{R}^T\dot{\mathbf{c}} - \mathbf{v} - \mathbf{S}(r)\Delta = 0. \tag{2.50}$$

From equation (2.50), the only variables actually controlled in this model are the linear and angular velocities (which are calculated respectively from the linear and angular accelerations after an integration). So, it is useful to study the dynamics of these variables depending on the leader's path and the displacement Δ. Let's consider a leader describing a path modelled similarly to the follower's, such that its velocity can be written as

$$\dot{\mathbf{c}} = C\left(\cos\psi_c\mathbf{e}_1 + \sin\psi_c\mathbf{e}_2\right), \tag{2.51}$$

where C and ψ_c are the leader's speed and heading angle, respectively, at each time instant. Following this reasoning, equation (2.50) can be simplified as

$$\begin{aligned}
&\begin{pmatrix} \cos\psi & -\sin\psi \\ \sin\psi & \cos\psi \end{pmatrix}^T C \begin{pmatrix} \cos\psi_c \\ \sin\psi_c \end{pmatrix} - \begin{pmatrix} v \\ 0 \end{pmatrix} - \begin{pmatrix} 0 & -r \\ r & 0 \end{pmatrix} \begin{pmatrix} \Delta_x \\ \Delta_y \end{pmatrix} = \begin{pmatrix} 0 \\ 0 \end{pmatrix} \\
\Leftrightarrow &\begin{pmatrix} v - r\Delta_y \\ r\Delta_x \end{pmatrix} = C \begin{pmatrix} \cos\psi & \sin\psi \\ -\sin\psi & \cos\psi \end{pmatrix} \begin{pmatrix} \cos\psi_c \\ \sin\psi_c \end{pmatrix} \\
\Leftrightarrow &\begin{pmatrix} 1 & -\Delta_y \\ 0 & \Delta_x \end{pmatrix} \begin{pmatrix} v \\ r \end{pmatrix} = C \begin{pmatrix} \cos\psi\cos\psi_c + \sin\psi\sin\psi_c \\ \cos\psi\sin\psi_c - \sin\psi\cos\psi_c \end{pmatrix} \\
\Leftrightarrow &\begin{pmatrix} v \\ r \end{pmatrix} = \frac{C}{\Delta_x} \begin{pmatrix} \Delta_x & \Delta_y \\ 0 & 1 \end{pmatrix} \begin{pmatrix} \cos(\psi - \psi_c) \\ \sin(\psi_c - \psi) \end{pmatrix} \\
\Leftrightarrow &\begin{pmatrix} v \\ r \end{pmatrix} = \frac{C}{\Delta_x} \begin{pmatrix} \Delta_x \cos(\psi - \psi_c) + \Delta_y \sin(\psi_c - \psi) \\ \sin(\psi_c - \psi) \end{pmatrix} \\
\Leftrightarrow &\begin{pmatrix} v \\ r \end{pmatrix} = \begin{pmatrix} C\cos(\psi - \psi_c) - \dfrac{C\Delta_y}{\Delta_x}\sin(\psi - \psi_c) \\ -\dfrac{C}{\Delta_x}\sin(\psi - \psi_c) \end{pmatrix} \quad ,\forall \Delta_x \neq 0.
\end{aligned} \tag{2.52}$$

These equations represent the closed loop and can be seen as describing a nonlinear system with a dynamics for ψ and an output v. If the heading difference is assumed to be very small, it can be approximated by a first-order system as

$$\dot{\psi} = -\frac{C}{\Delta_x}\left(\psi - \psi_c\right). \tag{2.53}$$

By taking the Laplace Transform on both sides one can represent the system in the frequency domain as

$$\begin{aligned}
s\Psi(s) &= -\frac{C}{\Delta_x}\left(\Psi(s) - \Psi_c(s)\right) \\
\Leftrightarrow \frac{\Psi(s)}{\Psi_c(s)} &= \frac{\frac{C}{\Delta_x}}{s + \frac{C}{\Delta_x}}.
\end{aligned} \tag{2.54}$$

Stability in ensured if

$$\frac{C}{\Delta_x} > 0 \Leftrightarrow \Delta_x > 0. \tag{2.55}$$

A physical interpretation of this result is that the leader must be seen by the follower from behind when they both head approximately in the same direction, which means the leader has to be always advanced in relation to the follower.

A more complete comprehension of the system can be achieved if the nonlinearities are taken into account. The equilibrium points of the system from equation (2.52) are

$$\psi^* = \psi_c + k\pi \quad ,\forall k \in \mathbb{Z}. \tag{2.56}$$

To analyse stability, one can consider infinitesimal disturbances around these equilibrium points. Let

$$\psi = \psi_c + 2k\pi + \epsilon \quad , \epsilon > 0. \tag{2.57}$$

Then, system (2.52) becomes

$$\begin{aligned} \dot{\psi} &= -\frac{C}{\Delta_x}\sin(2k\pi + \epsilon) \\ &= -\frac{C}{\Delta_x}\sin(\epsilon) \\ &\approx -\frac{C}{\Delta_x}\epsilon, \end{aligned} \tag{2.58}$$

which is negative if $\Delta_x > 0$. Thus, the system is asymptotically stable in the vicinity $\epsilon > 0$ of the equilibrium points $\psi^* = \psi_c + 2k\pi \quad , \forall k \in \mathbb{Z}$.

Similarly, if we consider

$$\psi = \psi_c + (2k+1)\pi + \epsilon \quad , \epsilon > 0, \tag{2.59}$$

system (2.52) becomes

$$\begin{aligned} \dot{\psi} &= -\frac{C}{\Delta_x}\sin((2k+1)\pi + \epsilon) \\ &= \frac{C}{\Delta_x}\sin(\epsilon) \\ &\approx \frac{C}{\Delta_x}\epsilon, \end{aligned} \tag{2.60}$$

which is positive if $\Delta_x > 0$. Thus, the system is unstable in the vicinity $\epsilon > 0$ of the equilibrium points $\psi^* = \psi_c + (2k+1)\pi \quad , \forall k \in \mathbb{Z}$.

A phase portrait of the system when $\psi_c = 0$ is represented in figure 2.2. It is easy to see that the region of convergence of the equilibrium point $\psi^* = \psi_c + 2k\pi$ is

$$\psi \in]\psi_c + (2k-1)\pi;\, \psi_c + (2k+1)\pi[\quad , \forall k \in \mathbb{Z}. \tag{2.61}$$

As a result, the follower can have a heading difference relative to the leader of up to $180°$. The bigger it is, the slower is the convergence to the desired heading. In the limit, if a follower is set to track a leader describing a linear path, starting in opposite heading, it will not converge.

2.3 3D motion

In § 2.2 the motion of the quadrotor at constant height has been studied and a controller for the simplified model has been derived through the backstepping method applied to the position error. We now wish to resort to the backstepping method to derive a similar nonlinear controller for the complete model.

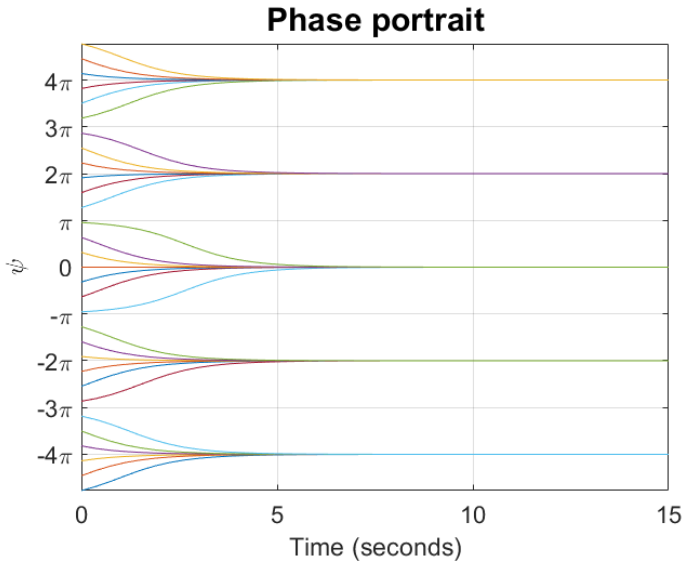

Figure 2.2: Phase portrait of the system $\dot{\psi} = -\sin(\psi)$.

2.3.1 State-space formulation

The first step prior to applying backstepping is to write the system in a special form. As done by [20], the complete quadrotor dynamics from equation (2.13) can be rewritten in a state-space form $\dot{X} = f(X, U)$ by introducing the state vector $X \in \mathbb{R}^{12}$ and the input vector $U \in \mathbb{R}^4$ given by

$$X = \begin{pmatrix} \phi & \dot{\phi} & \theta & \dot{\theta} & \psi & \dot{\psi} & z & \dot{z} & x & \dot{x} & y & \dot{y} \end{pmatrix}^T, \tag{2.62}$$

$$U = \begin{pmatrix} T & n_x & n_y & n_z \end{pmatrix}^T. \tag{2.63}$$

The nonlinear dynamics is

$$f(X,U) = \begin{pmatrix} \dot{\phi} \\ a_\phi \dot{\theta}\dot{\psi} + b_\phi n_x \\ \dot{\theta} \\ a_\theta \dot{\phi}\dot{\psi} + b_\theta n_y \\ \dot{\psi} \\ a_\psi \dot{\phi}\dot{\theta} + b_\psi n_z \\ \dot{z} \\ g - \frac{T}{m}\cos\phi\cos\theta \\ \dot{x} \\ \frac{T}{m}u_x \\ \dot{y} \\ \frac{T}{m}u_y \end{pmatrix} \tag{2.64}$$

with

$$u_x = \cos\phi\sin\theta\cos\psi + \sin\phi\sin\psi; \quad u_y = \cos\phi\sin\theta\sin\psi - \sin\phi\cos\psi \tag{2.65}$$

and the following constants

$$a_\phi = \frac{J_y - J_z}{J_x}; \quad a_\theta = \frac{J_z - J_x}{J_y}; \quad a_\psi = \frac{J_x - J_y}{J_z}; \quad b_\phi = \frac{1}{J_x}; \quad b_\theta = \frac{1}{J_y}; \quad b_\psi = \frac{1}{J_z} \tag{2.66}$$

The system as it is posed highlights an important relation between the position and attitude of the quadrotor. In fact, the position components depend on the angles, however the opposite is not true. In other words, the way the position evolves is a consequence of the attitude of the quadrotor but the attitude is oblivious to its position. As seen from figure 2.3, the overall system can be thought of as the result of two semi-decoupled subsystems: the translation subsystem and the rotation subsystem – for which two controllers will be designed separately.

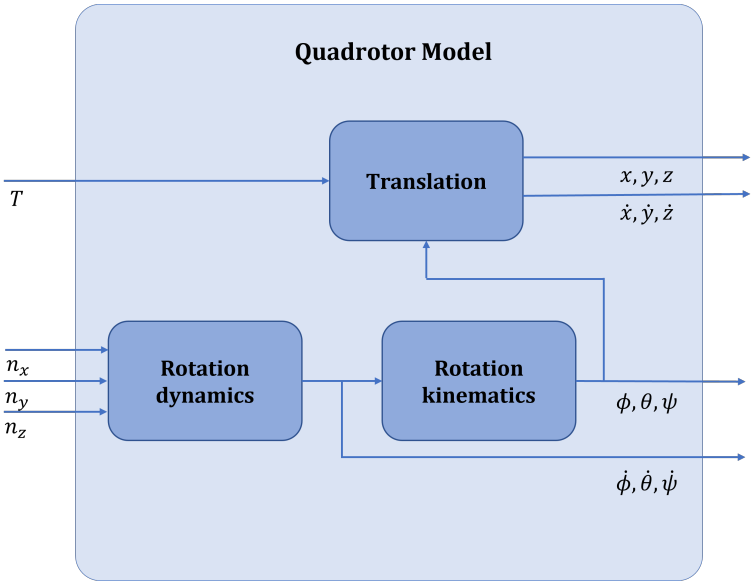

Figure 2.3: Quadrotor model scheme.

2.3.2 Attitude control

Roll

Let $z_\phi \in \mathbb{R}$ be the roll angle error given by

$$z_\phi = \phi_{\text{ref}} - \phi \tag{2.67}$$

and $V_\phi : \mathbb{R} \to \mathbb{R}$ a continuously differentiable Lyapunov function such that $V_\phi(0) = 0$, $V_\phi(z_\phi) > 0$, $\forall z_\phi \neq 0$ and $z_\phi \to \infty \Rightarrow V_\phi(z_\phi) \to \infty$ given by

$$V_\phi(z_\phi) = \frac{1}{2} z_\phi^2, \tag{2.68}$$

with its time derivative computed as

$$\dot{V}_\phi(z_\phi) = z_\phi \dot{z}_\phi = z_\phi(\dot{\phi}_{\text{ref}} - \dot{\phi}). \tag{2.69}$$

If $\dot{\phi}$ is controlled to be

$$\dot{\phi} = \dot{\phi}_{\text{ref}} + k_\phi z_\phi, \tag{2.70}$$

then

$$\dot{V}_\phi(z_\phi) = -k_\phi z_\phi^2. \tag{2.71}$$

Let now $z_{\dot{\phi}} \in \mathbb{R}$ be the roll rate error given by

$$z_{\dot{\phi}} = \dot{\phi} - \dot{\phi}_{\text{ref}} - k_\phi z_\phi \tag{2.72}$$

and $V_{\dot{\phi}} : \mathbb{R}^2 \to \mathbb{R}$ a continuously differentiable Lyapunov function such that $V_{\dot{\phi}}(0) = 0$, $V_{\dot{\phi}}(z_\phi, z_{\dot{\phi}}) > 0$, $\forall (z_\phi, z_{\dot{\phi}}) \neq 0$ and $(z_\phi, z_{\dot{\phi}}) \to \infty \Rightarrow V_\phi(z_\phi, z_{\dot{\phi}}) \to \infty$ given by

$$V_{\dot{\phi}}(z_\phi, z_{\dot{\phi}}) = V_\phi(z_\phi) + \frac{1}{2} z_{\dot{\phi}}^2, \tag{2.73}$$

with its time derivative computed as

$$\begin{aligned} \dot{V}_{\dot{\phi}}(z_\phi, z_{\dot{\phi}}) &= \dot{V}_\phi(z_\phi) + z_{\dot{\phi}} \dot{z}_{\dot{\phi}} \\ &= -k_\phi z_\phi^2 + z_{\dot{\phi}} (\ddot{\phi} - \ddot{\phi}_{\text{ref}} - k_\phi \dot{z}_\phi) \\ &= -k_\phi z_\phi^2 + z_{\dot{\phi}} (a_\phi \dot{\theta} \dot{\psi} + b_\phi n_x - \ddot{\phi}_{\text{ref}} - k_\phi \dot{z}_\phi) \end{aligned} \tag{2.74}$$

If the control law for n_x is chosen to be

$$n_x = \frac{1}{b_\phi} (\ddot{\phi}_{\text{ref}} + k_\phi \dot{z}_\phi - a_\phi \dot{\theta} \dot{\psi} - k_{\dot{\phi}} z_{\dot{\phi}}), \tag{2.75}$$

then

$$\dot{V}_{\dot{\phi}}(z_\phi, z_{\dot{\phi}}) = -k_\phi z_\phi^2 - k_{\dot{\phi}} z_{\dot{\phi}}^2. \tag{2.76}$$

It is clear that $\dot{V}_{\dot{\phi}}(z_\phi, z_{\dot{\phi}}) < 0$, $\forall (z_\phi, z_{\dot{\phi}}) \neq 0$ if $k_\phi > 0$ and $k_{\dot{\phi}} > 0$. Thus, according to the Barbashin-Krasovskii theorem [19, theorem 4.2], the roll error system is globally asymptotically stable around its equilibrium point $(z_\phi, z_{\dot{\phi}}) = 0$.

Pitch

Let $z_\theta \in \mathbb{R}$ be the pitch angle error given by

$$z_\theta = \theta_{\text{ref}} - \theta \tag{2.77}$$

and $V_\theta : \mathbb{R} \to \mathbb{R}$ a continuously differentiable Lyapunov function such that $V_\theta(0) = 0$, $V_\theta(z_\theta) > 0$, $\forall z_\theta \neq 0$ and $z_\theta \to \infty \Rightarrow V_\theta(z_\theta) \to \infty$ given by

$$V_\theta(z_\theta) = \frac{1}{2} z_\theta^2, \tag{2.78}$$

with its time derivative computed as

$$\dot{V}_\theta(z_\theta) = z_\theta \dot{z}_\theta = z_\theta(\dot{\theta}_{\text{ref}} - \dot{\theta}). \tag{2.79}$$

If $\dot{\theta}$ is controlled to be

$$\dot{\theta} = \dot{\theta}_{\text{ref}} + k_\theta z_\theta, \tag{2.80}$$

then

$$\dot{V}_\theta(z_\theta) = -k_\theta z_\theta^2. \tag{2.81}$$

Let now $z_{\dot{\theta}} \in \mathbb{R}$ be the pitch rate error given by

$$z_{\dot{\theta}} = \dot{\theta} - \dot{\theta}_{\text{ref}} - k_\theta z_\theta \tag{2.82}$$

and $V_{\dot{\theta}} : \mathbb{R}^2 \to \mathbb{R}$ a continuously differentiable Lyapunov function such that $V_{\dot{\theta}}(0) = 0$, $V_{\dot{\theta}}(z_\theta, z_{\dot{\theta}}) > 0$, $\forall (z_\theta, z_{\dot{\theta}}) \neq 0$ and $(z_\theta, z_{\dot{\theta}}) \to \infty \Rightarrow V_\theta(z_\theta, z_{\dot{\theta}}) \to \infty$ given by

$$V_{\dot{\theta}}(z_\theta, z_{\dot{\theta}}) = V_\theta(z_\theta) + \frac{1}{2} z_{\dot{\theta}}^2, \tag{2.83}$$

with its time derivative computed as

$$\begin{aligned} \dot{V}_{\dot{\theta}}(z_\theta, z_{\dot{\theta}}) &= \dot{V}_\theta(z_\theta) + z_{\dot{\theta}} \dot{z}_{\dot{\theta}} \\ &= -k_\theta z_\theta^2 + z_{\dot{\theta}}(\ddot{\theta} - \ddot{\theta}_{\text{ref}} - k_\theta \dot{z}_\theta) \\ &= -k_\theta z_\theta^2 + z_{\dot{\theta}}(a_\theta \dot{\phi}\dot{\psi} + b_\theta n_y - \ddot{\theta}_{\text{ref}} - k_\theta \dot{z}_\theta) \end{aligned} \tag{2.84}$$

If the control law for n_y is chosen to be

$$n_y = \frac{1}{b_\theta}(\ddot{\theta}_{\text{ref}} + k_\theta \dot{z}_\theta - a_\theta \dot{\phi}\dot{\psi} - k_{\dot{\theta}} z_{\dot{\theta}}), \tag{2.85}$$

then

$$\dot{V}_{\dot{\theta}}(z_\theta, z_{\dot{\theta}}) = -k_\theta z_\theta^2 - k_{\dot{\theta}} z_{\dot{\theta}}^2. \tag{2.86}$$

It is clear that $\dot{V}_{\dot{\theta}}(z_\theta, z_{\dot{\theta}}) < 0, \forall (z_\theta, z_{\dot{\theta}}) \neq 0$ if $k_\theta > 0$ and $k_{\dot{\theta}} > 0$. Thus, according to the Barbashin-Krasovskii theorem [19, theorem 4.2], the pitch error system is globally asymptotically stable around its equilibrium point $(z_\theta, z_{\dot{\theta}}) = 0$.

Yaw

Let $z_\psi \in \mathbb{R}$ be the yaw angle error given by

$$z_\psi = \psi_{\text{ref}} - \psi \tag{2.87}$$

and $V_\psi : \mathbb{R} \to \mathbb{R}$ a continuously differentiable Lyapunov function such that $V_\psi(0) = 0$, $V_\psi(z_\psi) > 0$, $\forall z_\psi \neq 0$ and $z_\psi \to \infty \Rightarrow V_\psi(z_\psi) \to \infty$ given by

$$V_\psi(z_\psi) = \frac{1}{2} z_\psi^2, \tag{2.88}$$

with its time derivative computed as

$$\dot{V}_\psi(z_\psi) = z_\psi \dot{z}_\psi = z_\psi(\dot{\psi}_{\text{ref}} - \dot{\psi}). \tag{2.89}$$

If $\dot{\psi}$ is controlled to be

$$\dot{\psi} = \dot{\psi}_{\text{ref}} + k_\psi z_\psi, \tag{2.90}$$

then

$$\dot{V}_\psi(z_\psi) = -k_\psi z_\psi^2. \tag{2.91}$$

Let now $z_{\dot{\psi}} \in \mathbb{R}$ be the yaw rate error given by

$$z_{\dot{\psi}} = \dot{\psi} - \dot{\psi}_{\text{ref}} - k_\psi z_\psi \tag{2.92}$$

and $V_{\dot{\psi}} : \mathbb{R}^2 \to \mathbb{R}$ a continuously differentiable Lyapunov function such that $V_{\dot{\psi}}(0) = 0$, $V_{\dot{\psi}}(z_\psi, z_{\dot{\psi}}) > 0$, $\forall (z_\psi, z_{\dot{\psi}}) \neq 0$ and $(z_\psi, z_{\dot{\psi}}) \to \infty \Rightarrow V_\psi(z_\psi, z_{\dot{\psi}}) \to \infty$ given by

$$V_{\dot{\psi}}(z_\psi, z_{\dot{\psi}}) = V_\psi(z_\psi) + \frac{1}{2} z_{\dot{\psi}}^2, \tag{2.93}$$

with its time derivative computed as

$$\begin{aligned} \dot{V}_{\dot{\psi}}(z_\psi, z_{\dot{\psi}}) &= \dot{V}_\psi(z_\psi) + z_{\dot{\psi}} \dot{z}_{\dot{\psi}} \\ &= -k_\psi z_\psi^2 + z_{\dot{\psi}}(\ddot{\psi} - \ddot{\psi}_{\text{ref}} - k_\psi \dot{z}_\psi) \\ &= -k_\psi z_\psi^2 + z_{\dot{\psi}}(a_\psi \dot{\phi}\dot{\theta} + b_\psi n_z - \ddot{\psi}_{\text{ref}} - k_\psi \dot{z}_\psi) \end{aligned} \tag{2.94}$$

If the control law for n_z is chosen to be

$$n_z = \frac{1}{b_\psi}(\ddot{\psi}_{\text{ref}} + k_\psi \dot{z}_\psi - a_\psi \dot{\phi}\dot{\theta} - k_{\dot{\psi}} z_{\dot{\psi}}), \tag{2.95}$$

then

$$\dot{V}_{\dot{\psi}}(z_\psi, z_{\dot{\psi}}) = -k_\psi z_\psi^2 - k_{\dot{\psi}} z_{\dot{\psi}}^2. \tag{2.96}$$

It is clear that $\dot{V}_{\dot{\psi}}(z_\psi, z_{\dot{\psi}}) < 0$, $\forall (z_\psi, z_{\dot{\psi}}) \neq 0$ if $k_\psi > 0$ and $k_{\dot{\psi}} > 0$. Thus, according to the Barbashin-Krasovskii theorem [19, theorem 4.2], the yaw error system is globally asymptotically stable around its equilibrium point $(z_\psi, z_{\dot{\psi}}) = 0$.

*

Having done backstepping for all the angular variables, the attitude controller is summarised

as

$$\begin{cases} n_x = \frac{1}{b_\phi}\left(\ddot{\phi}_{\text{ref}} + k_\phi(\dot{\phi}_{\text{ref}} - \dot{\phi}) - a_\phi\dot{\theta}\dot{\psi} - k_{\dot{\phi}}[\dot{\phi} - \dot{\phi}_{\text{ref}} - k_\phi(\phi_{\text{ref}} - \phi)]\right) \\ n_y = \frac{1}{b_\theta}\left(\ddot{\theta}_{\text{ref}} + k_\theta(\dot{\theta}_{\text{ref}} - \dot{\theta}) - a_\theta\dot{\phi}\dot{\psi} - k_{\dot{\theta}}[\dot{\theta} - \dot{\theta}_{\text{ref}} - k_\theta(\theta_{\text{ref}} - \theta)]\right) \\ n_z = \frac{1}{b_\psi}\left(\ddot{\psi}_{\text{ref}} + k_\psi(\dot{\psi}_{\text{ref}} - \dot{\psi}) - a_\psi\dot{\phi}\dot{\theta} - k_{\dot{\psi}}[\dot{\psi} - \dot{\psi}_{\text{ref}} - k_\psi(\psi_{\text{ref}} - \psi)]\right) \end{cases} . \tag{2.97}$$

In order to output the necessary moments, this controller receives as inputs the reference Euler angles and their derivatives up to the second and also the actual quadrotor attitude and angular velocity. As it will be shown further ahead in this work, the reference roll and pitch will be produced by the position controller, whereas the reference yaw is defined from the outset.

As stated in § 2.1, the quadrotor kinematics is well defined for any $\theta \neq (2k+1)\frac{\pi}{2}$, $\forall\, k \in \mathbb{Z}$. It is important to remember that, because of the singularities of the Euler angles and the topological limitations of SO(3) group, this attitude controller is almost globally stable.

2.3.3 Position control

A similar backstepping approach will next be followed for controlling the quadrotor position.

Altitude

Let $z_z \in \mathbb{R}$ be the altitude error given by

$$z_z = z_{\text{ref}} - z \tag{2.98}$$

and $V_z : \mathbb{R} \to \mathbb{R}$ a continuously differentiable Lyapunov function such that $V_z(0) = 0$, $V_z(z_z) > 0$, $\forall z_z \neq 0$ and $z_z \to \infty \Rightarrow V_z(z_z) \to \infty$ given by

$$V_z(z_z) = \frac{1}{2}z_z^2, \tag{2.99}$$

with its time derivative computed as

$$\dot{V}_z(z_z) = z_z\dot{z}_z = z_z(\dot{z}_{\text{ref}} - \dot{z}). \tag{2.100}$$

If $\dot{z}$ is controlled to be

$$\dot{z} = \dot{z}_{\text{ref}} + k_z z_z, \tag{2.101}$$

then

$$\dot{V}_z(z_z) = -k_z z_z^2. \tag{2.102}$$

Let now $z_{\dot{z}} \in \mathbb{R}$ be the vertical speed error given by

$$z_{\dot{z}} = \dot{z} - \dot{z}_{\text{ref}} - k_z z_z \tag{2.103}$$

and $V_{\dot{z}} : \mathbb{R}^2 \to \mathbb{R}$ a continuously differentiable Lyapunov function such that $V_{\dot{z}}(0) = 0$, $V_{\dot{z}}(z_z, z_{\dot{z}}) >$

0, $\forall(z_z, z_{\dot{z}}) \neq 0$ and $(z_z, z_{\dot{z}}) \to \infty \Rightarrow V_z(z_z, z_{\dot{z}}) \to \infty$ given by

$$V_{\dot{z}}(z_z, z_{\dot{z}}) = V_z(z_z) + \frac{1}{2} z_{\dot{z}}^2, \tag{2.104}$$

with its time derivative computed as

$$\begin{aligned} \dot{V}_{\dot{z}}(z_z, z_{\dot{z}}) &= \dot{V}_z(z_z) + z_{\dot{z}} \dot{z}_{\dot{z}} \\ &= -k_z z_z^2 + z_{\dot{z}}(\ddot{z} - \ddot{z}_{\text{ref}} - k_z \dot{z}_z) \\ &= -k_z z_z^2 + z_{\dot{z}} \left(g - \frac{T}{m} \cos\phi \cos\theta - \ddot{z}_{\text{ref}} - k_z \dot{z}_z \right) \end{aligned} \tag{2.105}$$

If the control law for T is chosen to be

$$T = \frac{m}{\cos\phi \cos\theta} (g - \ddot{z}_{\text{ref}} - k_z \dot{z}_z - k_{\dot{z}} z_{\dot{z}}), \tag{2.106}$$

then

$$\dot{V}_{\dot{z}}(z_z, z_{\dot{z}}) = -k_z z_z^2 - k_{\dot{z}} z_{\dot{z}}^2. \tag{2.107}$$

It is clear that $\dot{V}_{\dot{z}}(z_z, z_{\dot{z}}) < 0$, $\forall(z_z, z_{\dot{z}}) \neq 0$ if $k_z > 0$ and $k_{\dot{z}} > 0$. Thus, according to the Barbashin-Krasovskii theorem [19, theorem 4.2], the altitude error system is globally asymptotically stable around its equilibrium point $(z_z, z_{\dot{z}}) = 0$.

X position

Let $z_x \in \mathbb{R}$ be the x position error given by

$$z_x = x_{\text{ref}} - x \tag{2.108}$$

and $V_x : \mathbb{R} \to \mathbb{R}$ a continuously differentiable Lyapunov function such that $V_x(0) = 0$, $V_x(z_x) > 0$, $\forall z_x \neq 0$ and $z_x \to \infty \Rightarrow V_x(z_x) \to \infty$ given by

$$V_x(z_x) = \frac{1}{2} z_x^2, \tag{2.109}$$

with its time derivative computed as

$$\dot{V}_x(z_x) = z_x \dot{z}_x = z_x(\dot{x}_{\text{ref}} - \dot{x}). \tag{2.110}$$

If $\dot{x}$ is controlled to be

$$\dot{x} = \dot{x}_{\text{ref}} + k_x z_x, \tag{2.111}$$

then

$$\dot{V}_x(z_x) = -k_x z_x^2. \tag{2.112}$$

Let now $z_{\dot{x}} \in \mathbb{R}$ be the x speed error given by

$$z_{\dot{x}} = \dot{x} - \dot{x}_{\text{ref}} - k_x z_x \tag{2.113}$$

and $V_{\dot{x}} : \mathbb{R}^2 \to \mathbb{R}$ a continuously differentiable Lyapunov function such that $V_{\dot{x}}(0) = 0$, $V_{\dot{x}}(z_x, z_{\dot{x}}) > 0$, $\forall (z_x, z_{\dot{x}}) \neq 0$ and $(z_x, z_{\dot{x}}) \to \infty \Rightarrow V_x(z_x, z_{\dot{x}}) \to \infty$ given by

$$V_{\dot{x}}(z_x, z_{\dot{x}}) = V_x(z_x) + \frac{1}{2} z_{\dot{x}}^2, \tag{2.114}$$

with its time derivative computed as

$$\begin{aligned} \dot{V}_{\dot{x}}(z_x, z_{\dot{x}}) &= \dot{V}_x(z_x) + z_{\dot{x}} \dot{z}_{\dot{x}} \\ &= -k_x z_x^2 + z_{\dot{x}} (\ddot{x} - \ddot{x}_{\text{ref}} - k_x \dot{z}_x) \\ &= -k_x z_x^2 + z_{\dot{x}} \left(\frac{T}{m} u_x - \ddot{x}_{\text{ref}} - k_x \dot{z}_x \right) \end{aligned} \tag{2.115}$$

If the control law for u_x is chosen to be

$$u_x = \frac{m}{T} (\ddot{x}_{\text{ref}} + k_x \dot{z}_x - k_{\dot{x}} z_{\dot{x}}), \tag{2.116}$$

then

$$\dot{V}_{\dot{x}}(z_x, z_{\dot{x}}) = -k_x z_x^2 - k_{\dot{x}} z_{\dot{x}}^2. \tag{2.117}$$

It is clear that $\dot{V}_{\dot{x}}(z_x, z_{\dot{x}}) < 0$, $\forall (z_x, z_{\dot{x}}) \neq 0$ if $k_x > 0$ and $k_{\dot{x}} > 0$. Thus, according to the Barbashin-Krasovskii theorem [19, theorem 4.2], the x position error system is globally asymptotically stable around its equilibrium point $(z_x, z_{\dot{x}}) = 0$.

Y position

Let $z_y \in \mathbb{R}$ be the y position error given by

$$z_y = y_{\text{ref}} - y \tag{2.118}$$

and $V_y : \mathbb{R} \to \mathbb{R}$ a continuously differentiable Lyapunov function such that $V_y(0) = 0$, $V_y(z_y) > 0$, $\forall z_y \neq 0$ and $z_y \to \infty \Rightarrow V_y(z_y) \to \infty$ given by

$$V_y(z_y) = \frac{1}{2} z_y^2, \tag{2.119}$$

with its time derivative computed as

$$\dot{V}_y(z_y) = z_y \dot{z}_y = z_y (\dot{y}_{\text{ref}} - \dot{y}). \tag{2.120}$$

If $\dot{y}$ is controlled to be

$$\dot{y} = \dot{y}_{\text{ref}} + k_y z_y, \tag{2.121}$$

then

$$\dot{V}_y(z_y) = -k_y z_y^2. \tag{2.122}$$

Let now $z_{\dot{y}} \in \mathbb{R}$ be the y speed error given by

$$z_{\dot{y}} = \dot{y} - \dot{y}_{\text{ref}} - k_y z_y \tag{2.123}$$

and $V_{\dot{y}} : \mathbb{R}^2 \to \mathbb{R}$ a continuously differentiable Lyapunov function such that $V_{\dot{y}}(0) = 0$, $V_{\dot{y}}(z_y, z_{\dot{y}}) > 0$, $\forall (z_y, z_{\dot{y}}) \neq 0$ and $(z_y, z_{\dot{y}}) \to \infty \Rightarrow V_y(z_y, z_{\dot{y}}) \to \infty$ given by

$$V_{\dot{y}}(z_y, z_{\dot{y}}) = V_y(z_y) + \frac{1}{2} z_{\dot{y}}^2, \tag{2.124}$$

with its time derivative computed as

$$\begin{aligned} \dot{V}_{\dot{y}}(z_y, z_{\dot{y}}) &= \dot{V}_y(z_y) + z_{\dot{y}} \dot{z}_{\dot{y}} \\ &= -k_y z_y^2 + z_{\dot{y}} (\ddot{y} - \ddot{y}_{\text{ref}} - k_y \dot{z}_y) \\ &= -k_y z_y^2 + z_{\dot{y}} \left(\frac{T}{m} u_y - \ddot{y}_{\text{ref}} - k_y \dot{z}_y \right) \end{aligned} \tag{2.125}$$

If the control law for u_y is chosen to be

$$u_y = \frac{m}{T} (\ddot{y}_{\text{ref}} + k_y \dot{z}_y - k_{\dot{y}} z_{\dot{y}}), \tag{2.126}$$

then

$$\dot{V}_{\dot{y}}(z_y, z_{\dot{y}}) = -k_y z_y^2 - k_{\dot{y}} z_{\dot{y}}^2. \tag{2.127}$$

It is clear that $\dot{V}_{\dot{y}}(z_y, z_{\dot{y}}) < 0$, $\forall (z_y, z_{\dot{y}}) \neq 0$ if $k_y > 0$ and $k_{\dot{y}} > 0$. Thus, according to the Barbashin-Krasovskii theorem [19, theorem 4.2], the y position error system is globally asymptotically stable around its equilibrium point $(z_y, z_{\dot{y}}) = 0$.

*

The position controller is thus written as

$$\begin{cases} T = \frac{m}{\cos\phi \cos\theta} \left(g - \ddot{z}_{\text{ref}} - k_z (\dot{z}_{\text{ref}} - \dot{z}) - k_{\dot{z}} [\dot{z} - \dot{z}_{\text{ref}} - k_z (z_{\text{ref}} - z)] \right) \\ u_x = \frac{m}{T} \left(\ddot{x}_{\text{ref}} + k_x (\dot{x}_{\text{ref}} - \dot{x}) - k_{\dot{x}} [\dot{x} - \dot{x}_{\text{ref}} - k_x (x_{\text{ref}} - x)] \right) \\ u_y = \frac{m}{T} \left(\ddot{y}_{\text{ref}} + k_y (\dot{y}_{\text{ref}} - \dot{y}) - k_{\dot{y}} [\dot{y} - \dot{y}_{\text{ref}} - k_y (y_{\text{ref}} - y)] \right) \end{cases} . \tag{2.128}$$

Similarly enough to the attitude controller, this controller receives as inputs the reference position and its derivatives up to the second and also the actual quadrotor position and velocity. It outputs the required total thrust and the orientation of that vector responsible for the horizontal movement.

In order to feed the attitude controller with the reference values for roll and pitch, the definitions (2.65) are recalled and written in the following format:

$$\begin{pmatrix} u_x \\ u_y \end{pmatrix} = \begin{pmatrix} \cos\psi & \sin\psi \\ \sin\psi & -\cos\psi \end{pmatrix} \begin{pmatrix} A \\ B \end{pmatrix}, \tag{2.129}$$

where A and B are auxiliary variables defined as

$$A = \cos\phi \sin\theta; \quad B = \sin\phi. \tag{2.130}$$

This system is always invertible for any ψ defined from the outset so the reference roll and pitch can be calculated through the system of equations

$$\begin{cases} A^2 + B^2 = (1 - \sin^2\phi)\sin^2\theta + \sin^2\phi \\ \dfrac{B^2}{A^2} = \dfrac{\sin^2\phi}{(1 - \sin^2\phi)\sin^2\theta} \end{cases}. \tag{2.131}$$

Although this system of equations can be solved for appropriate values of ϕ_{ref} and θ_{ref}, it is highly nonlinear and multiple solutions are possible. To avoid any singularities and reduce the computational burden of these calculations, a simplified system is considered under the assumption that the quadrotor does not perform complex manoeuvres thereby keeping the roll and pitch angles small enough. In this case, $A \approx \theta$ and $B \approx \phi$ and the inputs of the attitude controller are

$$\begin{pmatrix} \theta_{\text{ref}} \\ \phi_{\text{ref}} \end{pmatrix} = \begin{pmatrix} \cos\psi & \sin\psi \\ \sin\psi & -\cos\psi \end{pmatrix} \begin{pmatrix} u_x \\ u_y \end{pmatrix}. \tag{2.132}$$

The attitude controller also requires the derivative and second derivative of the reference Euler angles. These derivatives could be explicitly computed from systems (2.129) or (2.132), however that would require measurements of the acceleration and its derivative, which are in all likelihood unavailable. A numerical differentiation of the reference angles is suggested by [21] and adapted to

$$\dot{\phi}_{\text{ref}} \approx \frac{\phi_{\text{ref}}(t) - \phi_{\text{ref}}(t - \Delta t)}{\Delta t}, \tag{2.133}$$

$$\dot{\theta}_{\text{ref}} \approx \frac{\theta_{\text{ref}}(t) - \theta_{\text{ref}}(t - \Delta t)}{\Delta t}, \tag{2.134}$$

where Δt is the sampling period. The second derivative of the reference angles can be computed likewise. Figure 2.4 depicts the control scheme for the 3D model.

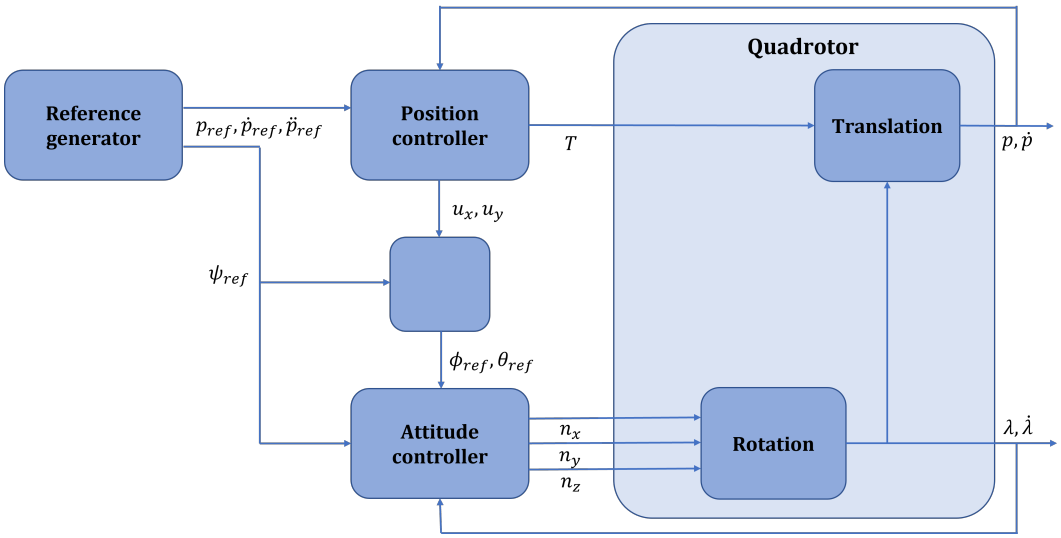

Figure 2.4: 3D controller scheme: position controller (2.128), attitude controller (2.97) and virtual output converter (2.132).

Chapter 3

Simulation results

3.1 2D simulations

This section shows the simulation results of a formation of two vehicles – one leader and one follower – in the two-dimensional space. The follower is intended to track a leader with four different trajectories for a simulation of 50 seconds. Table 3.1 contains the controller gains used for all simulations.

2D controller gains	
k_1	0.5 s^{-1}
k_2	0.5 s^{-1}
k_d	0.5

Table 3.1: 2D controller gains.

3.1.1 Still leader

In the first simulation, the leader stays still at the origin as the follower approaches keeping a displacement of $\Delta = (1, 1)$ m. The follower's initial position is $(5, 5)$ m, its initial heading is $\psi_0 = -90°$ and the disturbance intensity is $d = (1, 1)$ m/s^2. The simulation results are plotted in figure 3.1.

3.1.2 Linear tracking

In the second simulation, the leader describes a linear path departing from the origin. The follower's initial position is $(5, 5)$ m, its initial heading is $\psi_0 = 0°$, it keeps a displacement of $\Delta = (1, 1)$ m and the disturbance intensity is $d = (1, 1)$ m/s^2. The simulation results are plotted in figure 3.2.

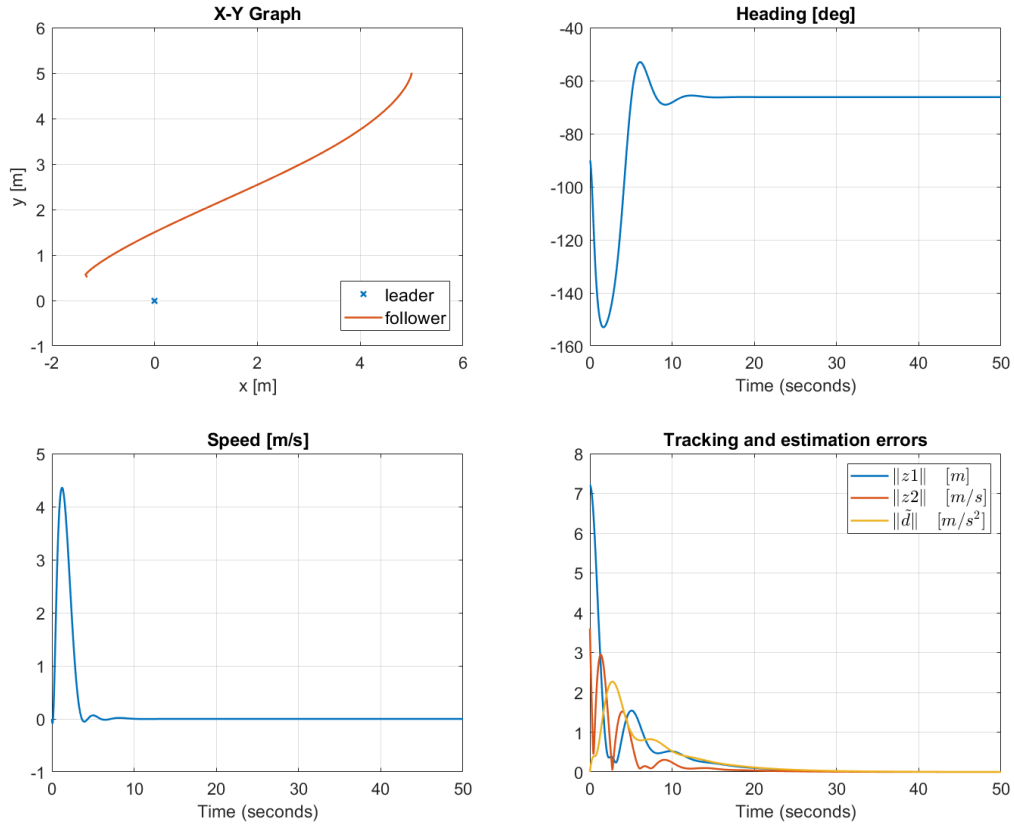

Figure 3.1: 2D simulation of a vehicle following a still leader with disturbance.

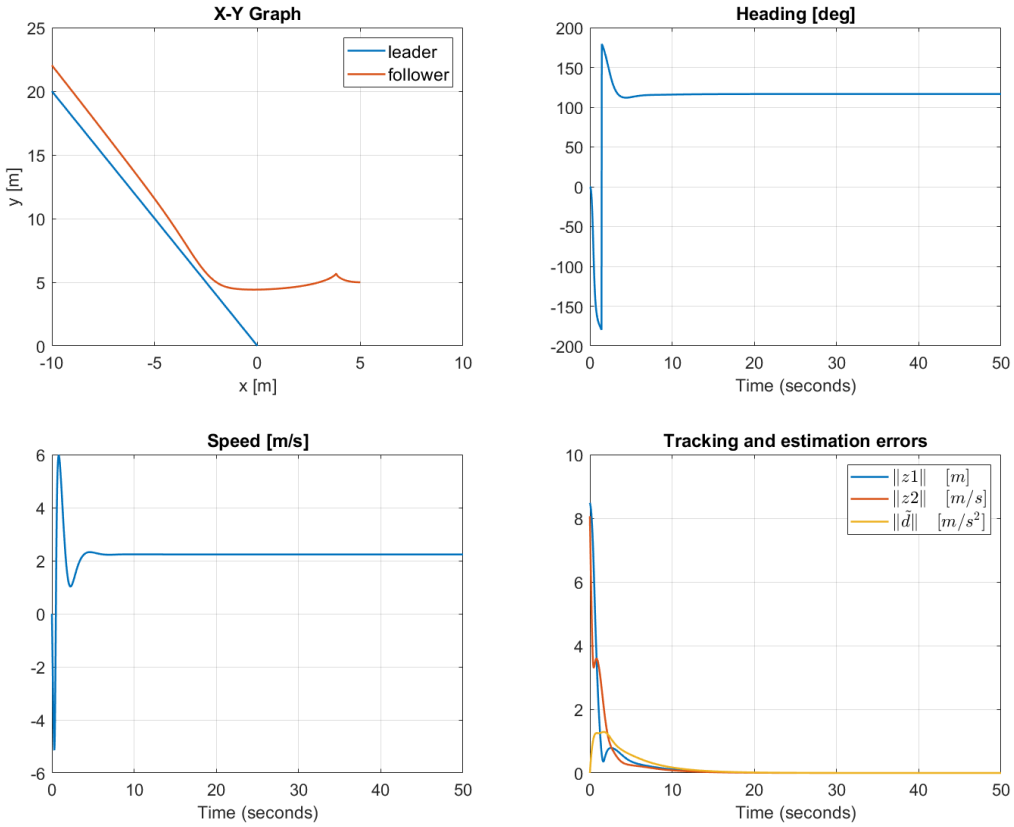

Figure 3.2: 2D simulation of a vehicle following a leader in a linear path with disturbance.

3.1.3 Circular tracking

In the third simulation, the leader describes a circular path with radius 2 meters and angular speed 1 m/s. The follower's initial position is $(3, 2)$ m, its initial heading is $\psi_0 = 90°$, it keeps a displacement of $\Delta = (1, 1)$ m and the disturbance intensity is $d = (1, 1)$ m/s^2. The simulation results are plotted in figure 3.3.

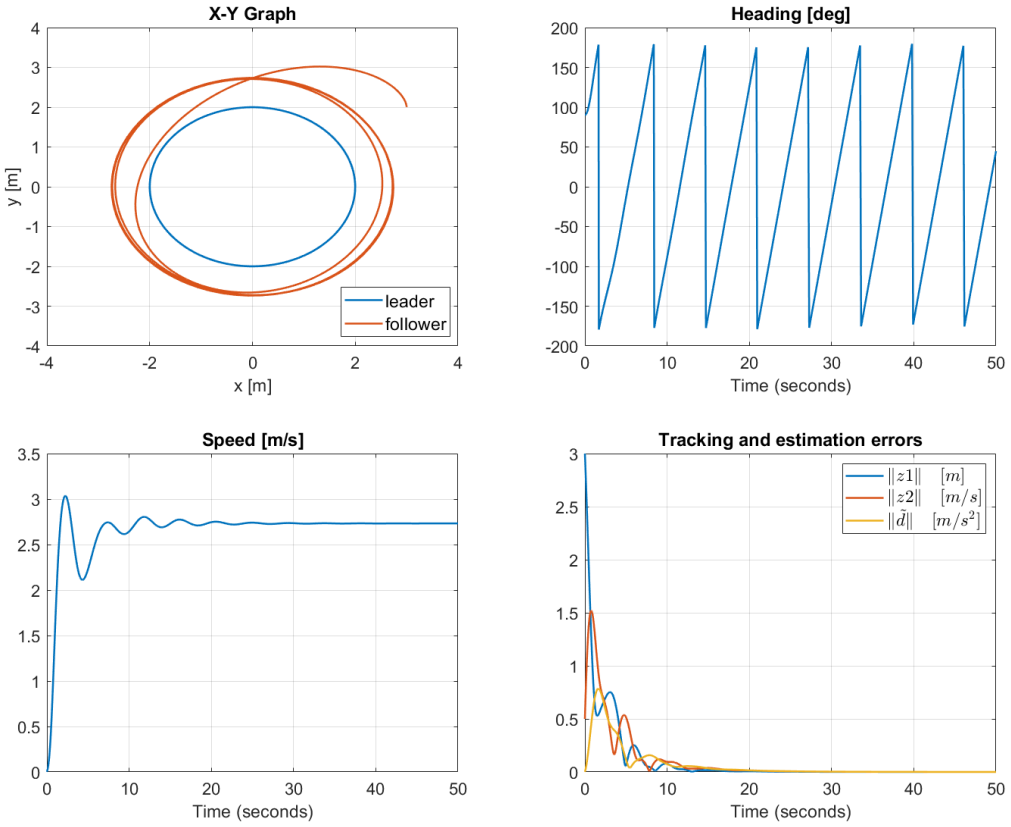

Figure 3.3: 2D simulation of a vehicle following a leader in a circular path with disturbance.

3.1.4 Sinusoidal tracking

In the third simulation, the leader describes a sinusoidal path departing from the origin. The follower's initial position is $(-10, 6)$ m, its initial heading is $\psi_0 = 0°$, it keeps a displacement of $\Delta = (0.5, 0.5)$ m and the disturbance intensity is $d = (1, 1)$ m/s^2. The simulation results are plotted in figure 3.4.

*

All the error plots from figures 3.1 to 3.4 show that both the position error z_1 and the velocity error z_2 converge to zero after around 10 to 20 seconds. Also, the disturbance estimation error $\tilde{d}$ converges to zero approximately at the same rate. This observation illustrates the proofs of convergence for the control law and adaptation law given in § 2.2.

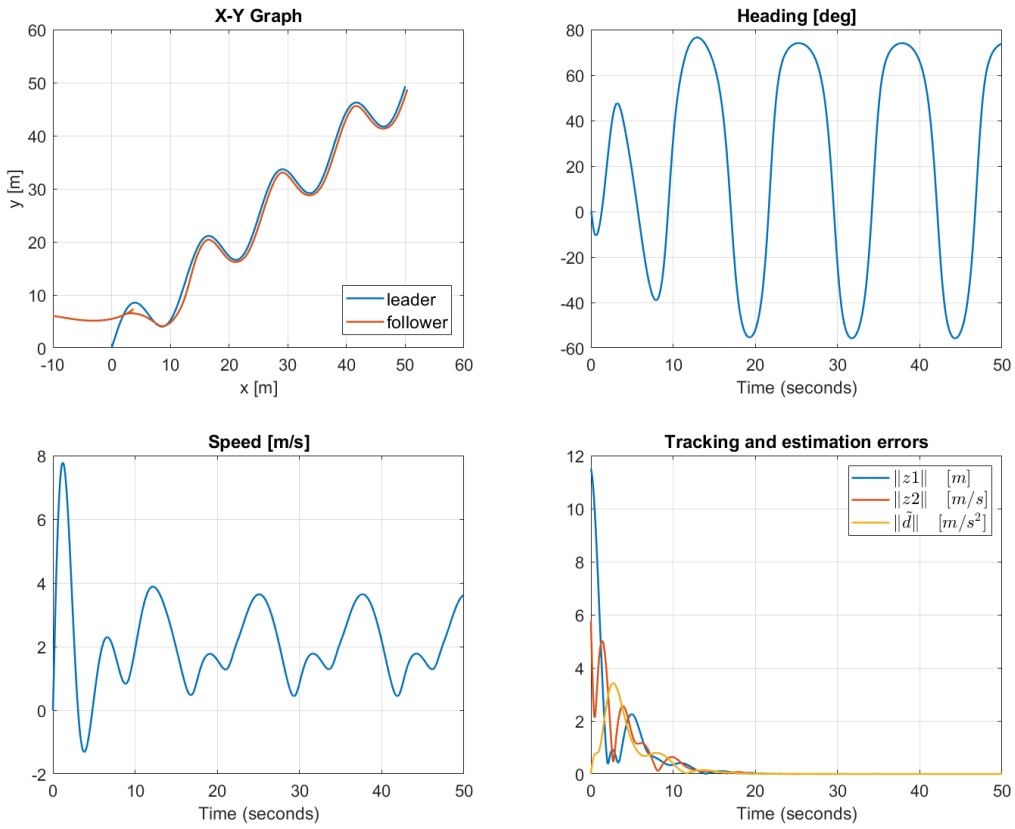

Figure 3.4: 2D simulation of a vehicle following a leader in a sinusoidal path with disturbance.

From the position plots, however, the displacement achieved by the formation in steady state is not so clear. This is due to the fact that the displacement has been expressed in the follower's body reference frame but the graphs are plotted in an inertial frame.

One final observation from the position and heading graphs is that the trajectory described by the follower prior to its convergence can be irregular and have sudden changes in the direction of movement. This behaviour is especially noticeable in figure 3.2 in the first 5 seconds of simulation.

3.2 3D simulations

This section shows the simulation results of a formation of two vehicles – one leader and one follower – in the three-dimensional space. Table 3.2 contains the physical characteristics of the quadrotors, namely its mass, radius, ratio between coefficient of torque and coefficient of thrust and moments of inertia. This values were obtained for the heavy quadrotor developed in [22], cited by [23].

The initial conditions of position, velocity, attitude and angular velocity of the follower vehicle have been made equal in all simulations and are shown in table 3.3. The simulations have been run for 100 seconds.

3D Model parameters	
m	4.34 kg
l	0.315 m
c_Q/c_T	8.004×10^{-4} m
J_x	0.0820 kg m^2
J_y	0.0845 kg m^2
J_z	0.1377 kg m^2

Table 3.2: Physical parameters of the 3D model [22].

3D Initial conditions	
(x_0, y_0, z_0)	$(0, 0, 0)$ m
(u_0, v_0, w_0)	$(0, 0, 0)$ m/s
$(\phi_0, \theta_0, \psi_0)$	$(0, 0, 0)$ rad
$(\dot{\phi}_0, \dot{\theta}_0, \dot{\psi}_0)$	$(0, 0, 0)$ rad/s

Table 3.3: Initial 3D simulation conditions.

3.2.1 Still leader

In the first simulation, the follower vehicle is intended to track a leader that stays still at position $(25, 35, 45)$ m while keeping the yaw angle equal to zero. The displacement to the leader should be $\Delta = (5, 5, 5)$ m. The controller gains are defined in table 3.4 and the simulations results are plotted in figure 3.5, including state variables, the distance to the leader and the actuation on each rotor.

Attitude			
k_ϕ	1 s^{-1}	$k_{\dot{\phi}}$	1 s^{-1}
k_θ	1 s^{-1}	$k_{\dot{\theta}}$	1 s^{-1}
k_ψ	1 s^{-1}	$k_{\dot{\psi}}$	1 s^{-1}
Position			
k_x	-0.5 s^{-1}	$k_{\dot{x}}$	0.05 s^{-1}
k_y	-0.5 s^{-1}	$k_{\dot{y}}$	0.05 s^{-1}
k_z	0.2 s^{-1}	$k_{\dot{z}}$	0.1 s^{-1}

Table 3.4: Controller gains for 3D still leader tracking.

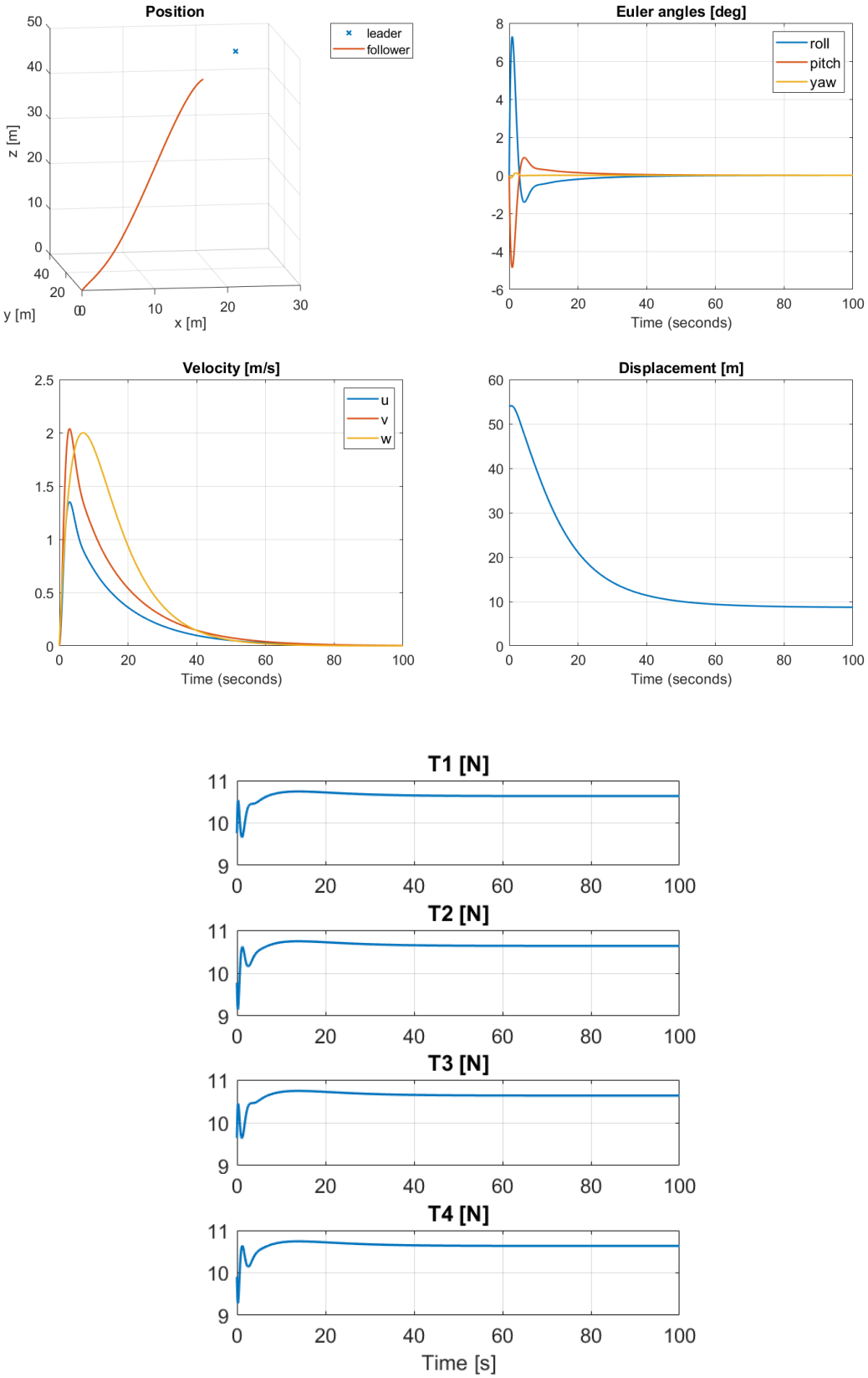

Figure 3.5: 3D simulation of a vehicle following a still leader.

3.2.2 Linear tracking

In the second simulation, the follower vehicle is intended to track a leader that describes a linear path starting at position $(5, 5, 25)$ m and moving at different speeds along the x, y and z axes. The follower should keep the yaw angle equal to zero. The displacement to the leader should be $\Delta = (5, 5, 5)$ m. The controller gains are defined in table 3.5 and the simulations results are plotted in figure 3.6, including state variables, the distance to the leader and the actuation on each rotor.

Attitude			
k_ϕ	1 s^{-1}	$k_{\dot{\phi}}$	1 s^{-1}
k_θ	1 s^{-1}	$k_{\dot{\theta}}$	1 s^{-1}
k_ψ	1 s^{-1}	$k_{\dot{\psi}}$	1 s^{-1}
Position			
k_x	-0.5 s^{-1}	$k_{\dot{x}}$	0.05 s^{-1}
k_y	-0.5 s^{-1}	$k_{\dot{y}}$	0.05 s^{-1}
k_z	0.2 s^{-1}	$k_{\dot{z}}$	0.1 s^{-1}

Table 3.5: Controller gains for 3D linear tracking.

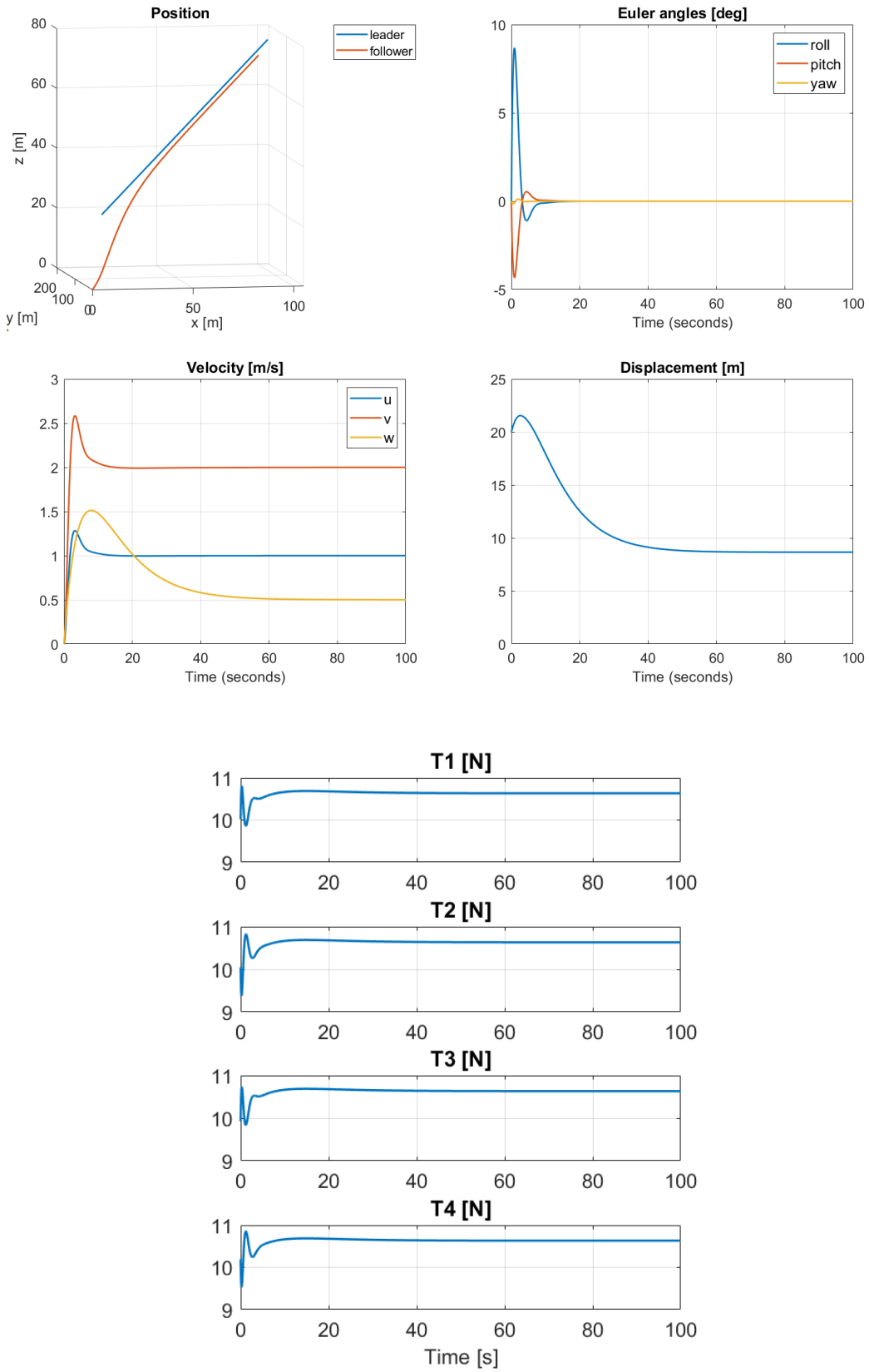

Figure 3.6: 3D simulation of a vehicle following a leader in a linear path.

3.2.3 Circular tracking with constant heading

In the third simulation, the follower vehicle is intended to track a leader that describes a circular path with radius 3 meters, angular speed 0.5 rad/s at constant height $z = 5$ m. The follower should keep the yaw angle equal to zero. The displacement to the leader should be $\Delta = (1, 1, 0)$ m. The controller gains are defined in table 3.6 and the simulations results are plotted in figure 3.7, including state variables, the distance to the leader and the actuation on each rotor.

Attitude			
k_ϕ	1 s^{-1}	$k_{\dot{\phi}}$	1 s^{-1}
k_θ	1 s^{-1}	$k_{\dot{\theta}}$	1 s^{-1}
k_ψ	1 s^{-1}	$k_{\dot{\psi}}$	1 s^{-1}
Position			
k_x	-2.2 s^{-1}	$k_{\dot{x}}$	0.18 s^{-1}
k_y	-2.2 s^{-1}	$k_{\dot{y}}$	0.18 s^{-1}
k_z	0.5 s^{-1}	$k_{\dot{z}}$	0.2 s^{-1}

Table 3.6: Controller gains for 3D circular tracking.

3.2.4 Circular tracking heading inwards

In the fourth simulation, the follower vehicle is intended to track the same leader as before but heading inwards. The yaw angle should change to make the quadrotor point to the centre of the trajectory. The controller gains are the same as defined in table 3.6 and the simulations results are plotted in figure 3.8, including state variables, the distance to the leader and the actuation on each rotor.

3.2.5 Circular tracking heading inwards with multiple followers and noise

A more ambitious simulation is done for a formation of one leader and two followers, each of them with equal controllers as defined in table 3.6 and departing from the same place. The first follower keeps a displacement of $\Delta_1 = (1, 1, 0)$ m and the second followers keeps a displacement of $\Delta_2 = (2, 2, 0)$. To add a little more reality into the simulation, white Gaussian noise is added to the sensors of the followers with signal-to-noise ratio equal to 45 dB. The simulation results are represented in figure 3.9.

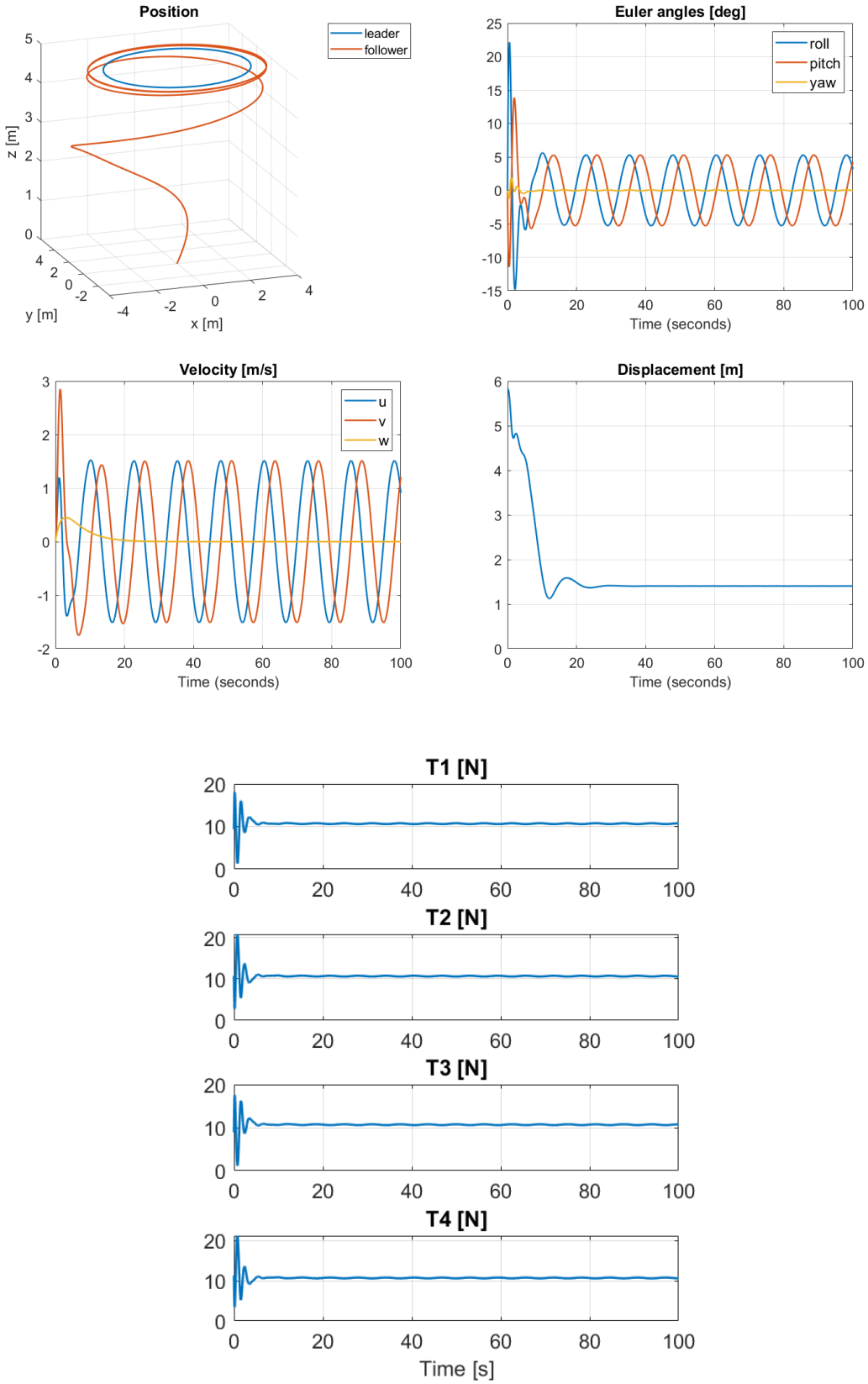

Figure 3.7: 3D simulation of a vehicle following a leader in a circular path with $\psi = 0$.

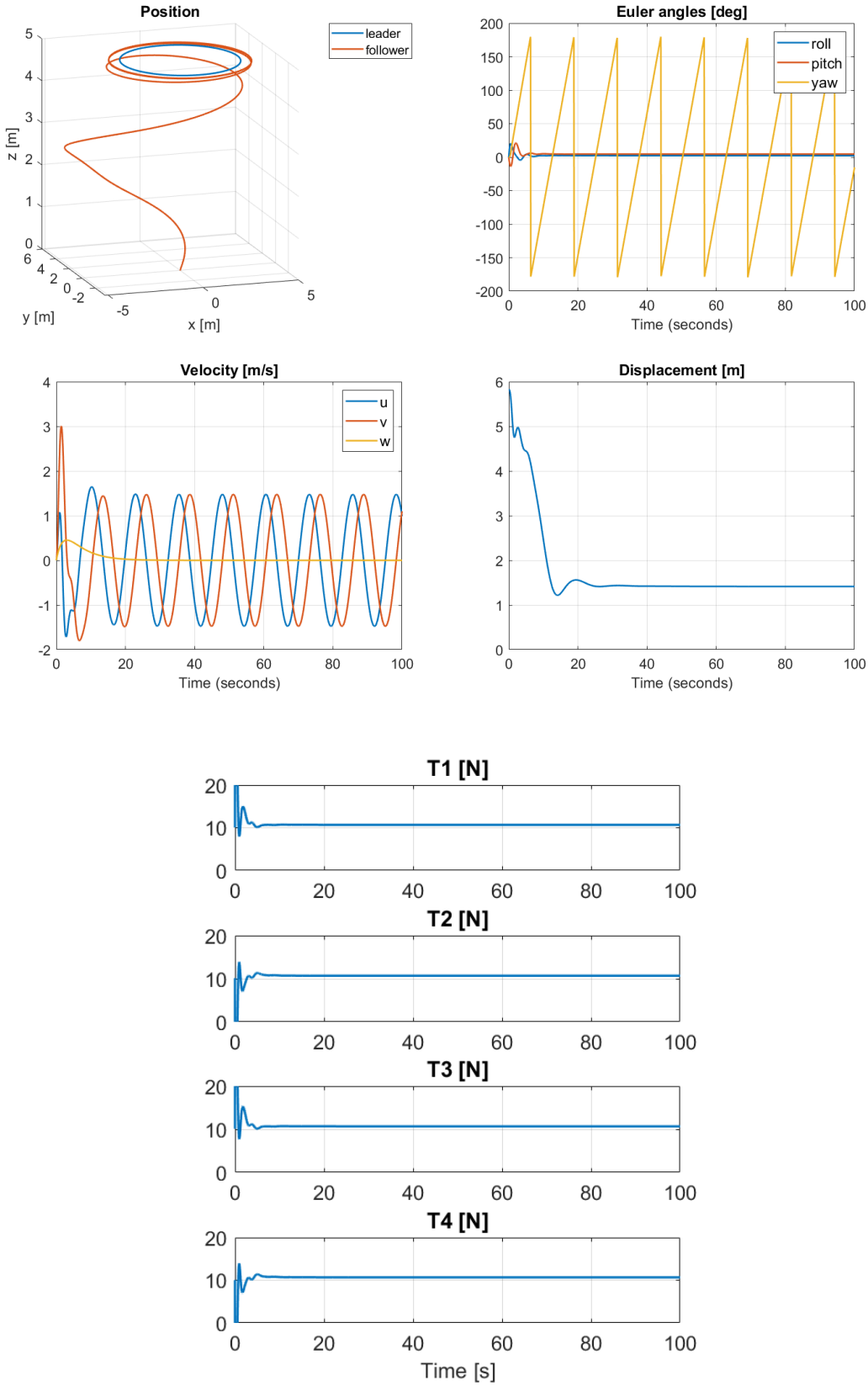

Figure 3.8: 3D simulation of a vehicle following a leader in a circular path heading inwards.

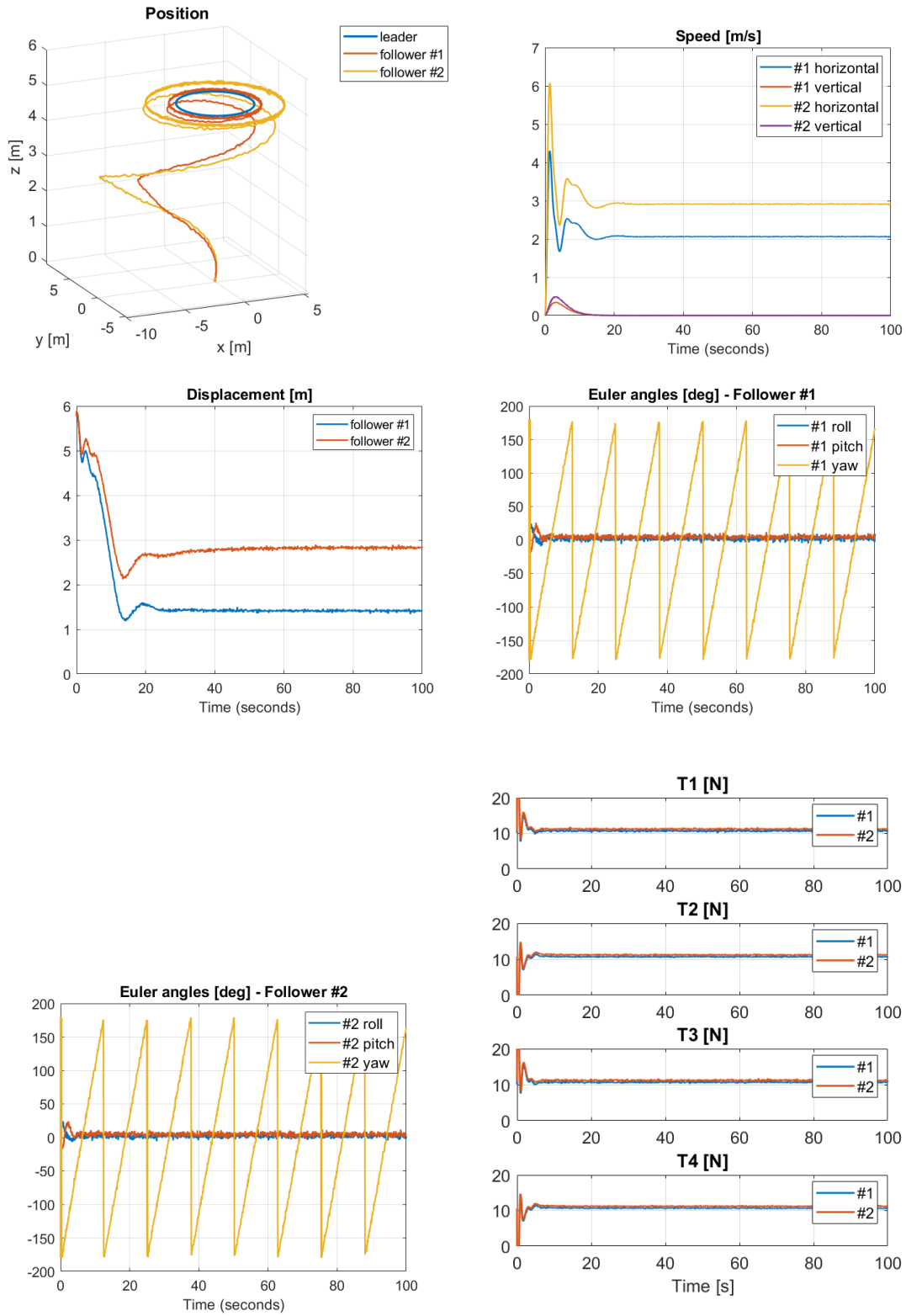

Figure 3.9: 3D simulation of two vehicles following a leader in a circular path heading inwards with noisy sensors.

*

As opposed to the error plots from § 3.1, the displacement plots from figures 3.5 to 3.9 show the distance from the follower(s) to the leader at each time instant. These plots converge to the

desired value after 20 to 40 seconds, which bears testimony to the fact that all position error systems converge to zero.

Also, the thrust forces for each rotor are represented and converge to a constant value when the movement is not accelerated. The main difference between the circular path simulations from figures 3.7 and 3.8 is the attitude and actuation. In the case of constant heading, the quadrotor has to continuously tilt and bank to describe the circular path. However, if the quadrotor adjusts to keep heading inwards, roll and pitch become constant. Taking a closer look at the angles in the second case, zoomed in in figure 3.10, it is possible to see that the vehicle can perform the curve with constant roll and pitch angles.

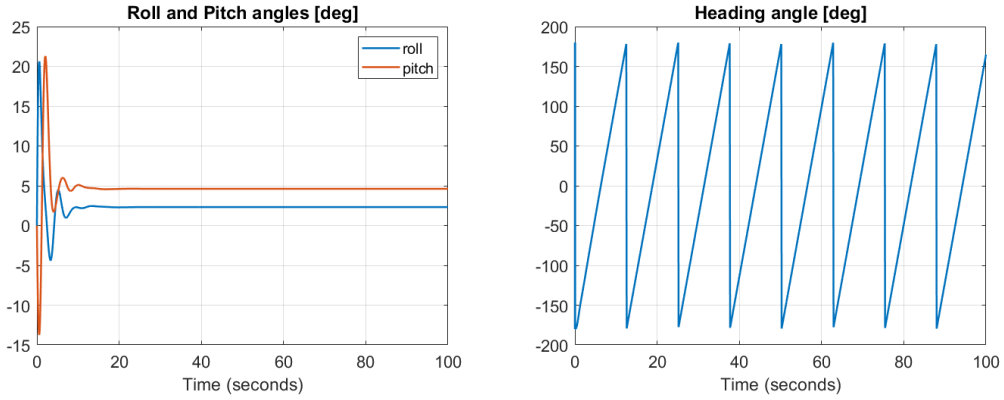

Figure 3.10: Attitude of the quadrotor in a circle heading inwards.

In what regards the simulation with two followers equipped with noisy sensors, it is made the assumption that the noise is both white and Gaussian. In fact, this assumption, however suitable for a simulation, is not completely correct. Firstly, the real noise is never completely white because the power spectral density is not necessarily constant for all frequencies. Secondly, the real noise is never completely Gaussian given that a Gaussian distribution allows infinite frequency values which is certainly not verifiable in a physical environment. The signal-to-noise ratio of 45 dB implies the power of the signal is more than 30 000 times higher than the power of noise, which might be rather optimistic.

Chapter 4

Conclusions

This work proposes an approach to the problem of flight formation by solving the trajectory tracking problem of quadrotor unmanned aerial vehicles. The formation is conceived as a leader vehicle being followed by a follower vehicle that keeps a constant displacement between them. The backstepping method has been applied to derive nonlinear control laws and the stability concerns have been addressed through Lyapunov stability theory.

The control solution is twofold. Firstly, only the motion at constant height was considered. In this case, the controller is purely kinematic but robust to constant acceleration disturbances and the stability of the error system is globally asymptotic. The dynamic behaviour of a closed-loop formation comprised of one leader and one follower is shown to be periodic. A formal proof of asymptotic stability within a certain region of convergence is also provided for this closed loop.

Secondly, a complete three-dimensional model was considered. This model is both kinematic and dynamic and takes into account the relevant inputs from the rotors spinning. The error system is also proved globally asymptotically stable.

Extensive simulation studies have been carried out to attest the performance of the control laws developed previously. For the motion at constant height, the follower was intended to track a still leader and a leader in a linear, circular and sinusoidal path. For the complete model, the follower tracks a still leader and a leader in a linear and circular path, with different heading requirements. At the end, a simulation has been carried out with two followers taking part in the formation with noisy measurements from the sensors.

4.1 Future Work

For the vastness and complexity of the formation control problem, never could this work aim to solve more than a small subproblem of the bigger problem. This work only considers simple formations of vehicles where the followers have complete access to the leader's position and velocity. One possible topic for future work, of special interest to large formations, could be addressing the problem of estimating variables unavailable to the followers.

The present solution is oblivious to any uninvited obstacles which may be found by the formation. In order to make the control solution more robust, incorporating collision avoidance techniques and adapting the formation framework could be another promising future development.

References

[1] T. Bacelar, C. Cardeira, and P. Oliveira, "Cooperative load transportation with quadrotors", in *2019 IEEE International Conference on Autonomous Robot Systems and Competitions (ICARSC)*, 2019, pp. 1–6. DOI: 10.1109/ICARSC.2019.8733619.

[2] M. Rosalie, J. E. Dentler, G. Danoy, P. Bouvry, S. Kannan, M. A. Olivares-Mendez, and H. Voos, "Area exploration with a swarm of uavs combining deterministic chaotic ant colony mobility with position mpc", in *2017 International Conference on Unmanned Aircraft Systems (ICUAS)*, 2017, pp. 1392–1397. DOI: 10.1109/ICUAS.2017.7991418.

[3] J. Scherer and B. Rinner, "Multi-uav surveillance with minimum information idleness and latency constraints", *IEEE Robotics and Automation Letters*, vol. 5, no. 3, pp. 4812–4819, 2020. DOI: 10.1109/LRA.2020.3003884.

[4] D. H. Stolfi, M. R. Brust, G. Danoy, and P. Bouvry, "A competitive predator–prey approach to enhance surveillance by uav swarms", *Applied Soft Computing*, vol. 111, p. 107 701, 2021, ISSN: 1568-4946. DOI: https://doi.org/10.1016/j.asoc.2021.107701.

[5] C. Ju and H. I. Son, "Multiple uav systems for agricultural applications: Control, implementation, and evaluation", *Electronics*, vol. 7, no. 9, 2018, ISSN: 2079-9292. DOI: 10.3390/electronics7090162.

[6] A. Das, R. Fierro, V. Kumar, J. Ostrowski, J. Spletzer, and C. Taylor, "A vision-based formation control framework", *IEEE Transactions on Robotics and Automation*, vol. 18, no. 5, pp. 813–825, 2002. DOI: 10.1109/TRA.2002.803463.

[7] J. Shao, G. Xie, and L. Wang, "Leader-following formation control of multiple mobile vehicles", *IET Control Theory and Applications*, vol. 1, no. 2, pp. 545–552, 2007. DOI: 10.1049/iet-cta:20050371.

[8] N. Leonard and E. Fiorelli, "Virtual leaders, artificial potentials and coordinated control of groups", in *Proceedings of the 40th IEEE Conference on Decision and Control (Cat. No.01CH37228)*, vol. 3, 2001, 2968–2973 vol.3. DOI: 10.1109/CDC.2001.980728.

[9] D. Lee, S. P. Viswanathan, L. Holguin, A. K. Sanyal, and E. A. Butcher, "Decentralized guidance and control for spacecraft formation flying using virtual leader configuration", in *2013 American Control Conference*, 2013, pp. 4826–4831. DOI: 10.1109/ACC.2013.6580585.

[10] T. Balch and R. Arkin, "Behavior-based formation control for multirobot teams", *IEEE Transactions on Robotics and Automation*, vol. 14, no. 6, pp. 926–939, 1998. DOI: 10.1109/70.736776.

[11] K.-K. Oh, M.-C. Park, and H.-S. Ahn, "A survey of multi-agent formation control", *Automatica*, vol. 53, pp. 424–440, 2015, ISSN: 0005-1098. DOI: https://doi.org/10.1016/j.automatica.2014.10.022.

[12] R. Olfati-Saber and R. Murray, "Consensus problems in networks of agents with switching topology and time-delays", *IEEE Transactions on Automatic Control*, vol. 49, no. 9, pp. 1520–1533, 2004. DOI: 10.1109/TAC.2004.834113.

[13] Z. Hou, W. Wang, G. Zhang, and C. Han, "A survey on the formation control of multiple quadrotors", in *2017 14th International Conference on Ubiquitous Robots and Ambient Intelligence (URAI)*, 2017, pp. 219–225. DOI: 10.1109/URAI.2017.7992717.

[14] W. Ren, R. W. Beard, and E. M. Atkins, "Information consensus in multivehicle cooperative control", *IEEE Control Systems Magazine*, vol. 27, no. 2, pp. 71–82, 2007. DOI: 10.1109/MCS.2007.338264.

[15] W. Ren, R. Beard, and E. Atkins, "A survey of consensus problems in multi-agent coordination", in *Proceedings of the 2005, American Control Conference, 2005.*, 2005, 1859–1864 vol. 3. DOI: 10.1109/ACC.2005.1470239.

[16] R. Olfati-Saber, "Flocking for multi-agent dynamic systems: Algorithms and theory", *IEEE Transactions on Automatic Control*, vol. 51, no. 3, pp. 401–420, 2006. DOI: 10.1109/TAC.2005.864190.

[17] I. Kaminer, A. Pascoal, E. Xargay, N. Hovakimyan, V. Cichella, and V. Dobrokhodov, *Time-Critical Cooperative Control of Autonomous Air Vehicles*. Butterworth-Heinemann, 2017.

[18] V. Cichella, I. Kaminer, V. Dobrokhodov, E. Xargay, R. Choe, N. Hovakimyan, A. P. Aguiar, and A. M. Pascoal, "Cooperative path following of multiple multirotors over time-varying networks", *IEEE Transactions on Automation Science and Engineering*, vol. 12, no. 3, pp. 945–957, 2015. DOI: 10.1109/TASE.2015.2406758.

[19] H. K. Khalil, *Nonlinear Systems*, 3rd edition. Pearson, 2014.

[20] S. Bouabdallah and R. Siegwart, "Backstepping and sliding-mode techniques applied to an indoor micro quadrotor", in *Proceedings of the 2005 IEEE International Conference on Robotics and Automation*, 2005, pp. 2247–2252. DOI: 10.1109/ROBOT.2005.1570447.

[21] R. Pérez-Alcocer, J. Moreno-Valenzuela, and R. Miranda-Colorado, "A robust approach for trajectory tracking control of a quadrotor with experimental validation", *ISA Transactions*, vol. 65, pp. 262–274, 2016, ISSN: 0019-0578. DOI: https://doi.org/10.1016/j.isatra.2016.08.001.

[22] P. Pounds, R. Mahony, and P. Corke, "Modelling and control of a large quadrotor robot", *Control Engineering Practice*, vol. 18, no. 7, pp. 691–699, 2010, Special Issue on Aerial Robotics, ISSN: 0967-0661. DOI: https://doi.org/10.1016/j.conengprac.2010.02.008.

[23] T. Lee, M. Leok, and N. H. McClamroch, "Geometric tracking control of a quadrotor uav on se(3)", in *49th IEEE Conference on Decision and Control (CDC)*, 2010, pp. 5420–5425. DOI: 10.1109/CDC.2010.5717652.